 doi:10.20944/preprints202209.0444.v1

Article

Reciprocity and representations for wave fields in 3D inhomogeneous parity-time symmetric materials

Kees Wapenaar[1], Evert Slob[2]

Department of Geoscience and Engineering, Delft University of Technology, The Netherlands;
[1]c.p.a.wapenaar@tudelft.nl, [2]e.c.slob@tudelft.nl

Abstract: Inspired by recent developments in wave propagation and scattering experiments with parity-time ($\mathcal{PT}$) symmetric materials, we discuss reciprocity and representation theorems for 3D inhomogeneous $\mathcal{PT}$-symmetric materials and indicate some applications. We start with a unified matrix-vector wave equation which accounts for acoustic, quantum-mechanical, electromagnetic, elastodynamic, poroelastodynamic, piezoelectric and seismoelectric waves. Based on the symmetry properties of the operator matrix in this equation, we derive unified reciprocity theorems for wave fields in 3D arbitrary inhomogeneous media and 3D inhomogeneous media with $\mathcal{PT}$-symmetry. These theorems form the basis for deriving unified wave field representations and relations between reflection and transmission responses in such media. Among the potential applications are interferometric Green's matrix retrieval and Marchenko-type Green's matrix retrieval in $\mathcal{PT}$-symmetric materials.

Keywords: parity-time symmetry; reciprocity; Green's matrix; metamaterials

1. Introduction

A parity-time ($\mathcal{PT}$) symmetric system is a physical system that is invariant under the combined reversal of the space and time coordinates. Having its roots in quantum physics [1], the principle of $\mathcal{PT}$-symmetry has recently found many applications in classical wave propagation and scattering problems in photonic structures [2–4], phononic crystals [5–7] and acoustic metamaterials [8–10]. Motivations for designing $\mathcal{PT}$-symmetric materials are the exotic properties that can be achieved, such as unidirectional optical wave propagation [11], negative refraction [10] and acoustic cloaking [8,9].

Reversal of the time coordinate of a dissipative (passive) material results in an effectual (active) material and vice-versa [12–14]. Hence, a $\mathcal{PT}$-symmetric medium is constructed from materials with loss and gain, balanced with respect to the origin of the spatial coordinate system. Natural materials are dissipative, but in specific situations waves may gain energy during propagation. For example, in photonics this occurs through two-wave mixing using the nonlinear photorefractive effect [2,15], whereas in phononic structures waves may gain energy through the acoustoelectric effect of piezoelectric semiconductors [5,16]. Another possibility is to construct $\mathcal{PT}$-symmetric materials by virtualising the effectual (active) part of such a medium. References [17–20] propose to construct virtual acoustic $\mathcal{PT}$-symmetric materials by connecting physical passive systems with numerical active systems via the principle of immersive wave experimentation [21–23].

In this paper we discuss reciprocity and representation theorems for wave fields in 3D inhomogeneous $\mathcal{PT}$-symmetric materials. In general, a wave-field reciprocity theorem interrelates two states (sources, medium parameters and wave fields) in one-and-the-same spatial domain [24–27]. We review two reciprocity theorems for wave fields in 3D arbitrary inhomogeneous media (one of the convolution type and one of the correlation type) and derive two new reciprocity theorems for 3D inhomogeneous media with $\mathcal{PT}$-symmetry. As the basis for these four reciprocity theorems we use a unified matrix-vector wave equation, which covers acoustic, quantum-mechanical, electromagnetic, elastodynamic, poroelastodynamic, piezoelectric and seismoelectric waves. Next, we derive wave field representations. In general, a wave field representation is obtained by replacing one of the

Citation: Wapenaar, K.; Slob, E. Reciprocity and representations for wave fields in 3D inhomogeneous parity-time symmetric materials. *Preprints* **2022**, *1*, 0. https://doi.org/10.3390/symxxx

Preprints (www.preprints.org) | NOT PEER-REVIEWED | Posted: 28 September 2022 doi:10.20944/preprints202209.0444.v1

states in a reciprocity theorem by a Green's state [28–31]. Among other results, we obtain a unified representation for interferometric Green's matrix retrieval in a 3D $\mathcal{PT}$-symmetric medium. Following an approach similar to reference [32], we also use the four reciprocity theorems to derive a number of relations between reflection and transmission responses for arbitrary inhomogeneous media and for $\mathcal{PT}$-symmetric media. One of the results is a generalisation to unified wave fields in 3D inhomogeneous $\mathcal{PT}$-symmetric media of the unitarity relation $|T|^2 = 1 - R_L^* R_R$ for scalar fields in a stratified $\mathcal{PT}$-symmetric medium [6,8]. Finally, we discuss the Marchenko method. In general, the Marchenko method provides a way to retrieve the Green's response between a point at the surface and a point inside the medium from the reflection response at the surface [33–35]. One of the underlying assumptions is that the medium is lossless. We show that this assumption can be circumvented when the medium is $\mathcal{PT}$-symmetric and the reflection response is available at two sides of the medium. We illustrate the Marchenko method for a layered medium with $\mathcal{PT}$-symmetry with a numerical example.

2. Unified matrix-vector wave equation

As the starting point for our derivations we consider the following unified matrix-vector wave equation [36–41]

$$\partial_3 \mathbf{q} - \boldsymbol{\mathcal{A}}\, \mathbf{q} = \mathbf{d}. \tag{1}$$

Here $\mathbf{q}(\mathbf{x}, \omega)$ is a $N \times 1$ wave-field vector, which is a function of space ($\mathbf{x}$) and angular frequency (ω), with the space coordinate vector defined as $\mathbf{x} = (x_1, x_2, x_3)$ (throughout this paper we assume that the x_3-axis is pointing downward). Similarly, $\mathbf{d}(\mathbf{x}, \omega)$ is a $N \times 1$ space- and frequency-dependent source vector. Operator ∂_3 stands for the partial differential operator $\partial/\partial x_3$. Finally, $\boldsymbol{\mathcal{A}}(\mathbf{x}, \omega, \partial_\alpha)$ is a $N \times N$ operator matrix, containing space- and frequency-dependent medium parameters (or, for quantum-mechanical waves, the potential) and operators ∂_α (standing for the partial differential operator $\partial/\partial x_\alpha$, with Greek subscript α taking the values 1 and 2). For the moment we consider an arbitrary inhomogeneous medium (or potential). The specifics for a $\mathcal{PT}$-symmetric medium are discussed later.

We partition $\mathbf{q}$, $\mathbf{d}$ and $\boldsymbol{\mathcal{A}}$ as follows

$$\mathbf{q} = \begin{pmatrix} \mathbf{q}_1 \\ \mathbf{q}_2 \end{pmatrix}, \quad \mathbf{d} = \begin{pmatrix} \mathbf{d}_1 \\ \mathbf{d}_2 \end{pmatrix}, \quad \boldsymbol{\mathcal{A}} = \begin{pmatrix} \boldsymbol{\mathcal{A}}_{11} & \boldsymbol{\mathcal{A}}_{12} \\ \boldsymbol{\mathcal{A}}_{21} & \boldsymbol{\mathcal{A}}_{22} \end{pmatrix}, \tag{2}$$

where sub-vectors $\mathbf{q}_1$, $\mathbf{q}_2$, $\mathbf{d}_1$ and $\mathbf{d}_2$ are $N/2 \times 1$ vectors and where sub-matrices $\boldsymbol{\mathcal{A}}_{11}$, $\boldsymbol{\mathcal{A}}_{12}$, $\boldsymbol{\mathcal{A}}_{21}$ and $\boldsymbol{\mathcal{A}}_{22}$ are $N/2 \times N/2$ operator matrices. Table 1 gives an overview of the wave-field sub-vectors $\mathbf{q}_1$ and $\mathbf{q}_2$ for different wave phenomena. These sub-vectors are organized such that the power-flux density j in the x_3-direction (or, for quantum-mechanical waves, the probability current density j) follows from

$$j = \frac{1}{4}(\mathbf{q}_1^\dagger \mathbf{q}_2 + \mathbf{q}_2^\dagger \mathbf{q}_1), \tag{3}$$

where superscript † denotes transposition and complex conjugation. The source sub-vectors and operator sub-matrices for all wave phenomena of Table 1 are reviewed or derived in reference [41], in most cases for anisotropic media.

Preprints (www.preprints.org) | NOT PEER-REVIEWED | Posted: 28 September 2022 doi:10.20944/preprints202209.0444.v1

Table 1. (After reference [41]). Wave-field sub-vectors $\mathbf{q}_1(\mathbf{x},\omega)$ and $\mathbf{q}_2(\mathbf{x},\omega)$ for different wave phenomena. For details see Appendix A.1.

	N	$\mathbf{q}_1$	$\mathbf{q}_2$
Acoustic	2	p	v_3
Quantum-mechanical	2	ψ	$\frac{2\hbar}{mi}\partial_3\psi$
Electromagnetic	4	$\mathbf{E}_0 = \begin{pmatrix} E_1 \\ E_2 \end{pmatrix}$	$\mathbf{H}_0 = \begin{pmatrix} H_2 \\ -H_1 \end{pmatrix}$
Elastodynamic	6	$\mathbf{v} = \begin{pmatrix} v_1 \\ v_2 \\ v_3 \end{pmatrix}$	$-\boldsymbol{\tau}_3 = -\begin{pmatrix} \tau_{13} \\ \tau_{23} \\ \tau_{33} \end{pmatrix}$
Poroelastodynamic	8	$\begin{pmatrix} \mathbf{v}^s \\ \phi(v_3^f - v_3^s) \end{pmatrix}$	$\begin{pmatrix} -\boldsymbol{\tau}_3^b \\ p^f \end{pmatrix}$
Piezoelectric	10	$\begin{pmatrix} \mathbf{v} \\ \mathbf{H}_0 \end{pmatrix}$	$\begin{pmatrix} -\boldsymbol{\tau}_3 \\ \mathbf{E}_0 \end{pmatrix}$
Seismoelectric	12	$\begin{pmatrix} \mathbf{v}^s \\ \phi(v_3^f - v_3^s) \\ \mathbf{H}_0 \end{pmatrix}$	$\begin{pmatrix} -\boldsymbol{\tau}_3^b \\ p^f \\ \mathbf{E}_0 \end{pmatrix}$

As an example, here we specify the $N/2 \times N/2$ operator sub-matrices for electromagnetic waves (for which $N = 4$) in an inhomogeneous, isotropic medium (other examples are given in Appendix A). They are defined as [42,43]

$$\boldsymbol{\mathcal{A}}_{12} = \begin{pmatrix} i\omega\mu - \frac{1}{i\omega}\partial_1\frac{1}{\varepsilon}\partial_1 & -\frac{1}{i\omega}\partial_1\frac{1}{\varepsilon}\partial_2 \\ -\frac{1}{i\omega}\partial_2\frac{1}{\varepsilon}\partial_1 & i\omega\mu - \frac{1}{i\omega}\partial_2\frac{1}{\varepsilon}\partial_2 \end{pmatrix}, \tag{4}$$

$$\boldsymbol{\mathcal{A}}_{21} = \begin{pmatrix} i\omega\mathcal{E} - \frac{1}{i\omega}\partial_2\frac{1}{\mu}\partial_2 & \frac{1}{i\omega}\partial_2\frac{1}{\mu}\partial_1 \\ \frac{1}{i\omega}\partial_1\frac{1}{\mu}\partial_2 & i\omega\mathcal{E} - \frac{1}{i\omega}\partial_1\frac{1}{\mu}\partial_1 \end{pmatrix}, \tag{5}$$

with

$$\mathcal{E} = \varepsilon + \frac{i\sigma}{\omega}, \tag{6}$$

where i is the imaginary unit, and $\boldsymbol{\mathcal{A}}_{11} = \boldsymbol{\mathcal{A}}_{22} = \mathbf{O}$, where $\mathbf{O}$ is a zero matrix (here it is a $N/2 \times N/2$ matrix, but at other places in this paper it is a $N \times N$ matrix; the size of this matrix is always clear from its context). Operator sub-matrices $\boldsymbol{\mathcal{A}}_{12}$ and $\boldsymbol{\mathcal{A}}_{21}$ contain the medium parameters $\varepsilon(\mathbf{x},\omega)$ (permittivity), $\mu(\mathbf{x},\omega)$ (permeability) and $\sigma(\mathbf{x},\omega)$ (conductivity), and differential operators ∂_α. The notation in the right-hand sides of equations (4) and (5) should be understood in the sense that differential operators act on all factors to the right of it. Hence, operator $\partial_1\frac{1}{\varepsilon}\partial_1$, applied via equation (1) to the magnetic field component H_2, stands for $\partial_1(\frac{1}{\varepsilon}\partial_1 H_2)$, etc. When the medium is dissipative, the medium parameters are frequency-dependent and complex-valued, with (for positive ω) $\Im(\varepsilon) > 0$, $\Im(\mu) > 0$, $\Re(\sigma) > 0$ and hence $\Im(\mathcal{E}) > 0$ (where $\Re$ stands for the real part and $\Im$ for the imaginary part). On the other hand, when the medium is effectual, we have (for positive ω) $\Im(\varepsilon) < 0$, $\Im(\mu) < 0$, $\Re(\sigma) < 0$ and hence $\Im(\mathcal{E}) < 0$. When a medium is dissipative, its adjoint is effectual, and vice versa. Adjoint medium parameters will be defined by an overbar. In particular, $\bar{\varepsilon} = \varepsilon^*$, $\bar{\mu} = \mu^*$, $\bar{\sigma} = -\sigma^*$ and hence $\bar{\mathcal{E}} = \mathcal{E}^*$, where superscript $*$ denotes complex conjugation. More generally, for the wave phenomena of Table 1, adjoint medium parameters are defined as the complex conjugate of the original parameters, except when a parameter is explicitly associated to dissipation (like σ), in which case the adjoint medium parameter is defined as minus the complex conjugate of the original parameter (next to the conductivity σ, this applies to the fluid viscosity η in porous

Preprints (www.preprints.org) | NOT PEER-REVIEWED | Posted: 28 September 2022 doi:10.20944/preprints202209.0444.v1

media and to Onsager's coupling coefficient L for seismoelectric waves, hence, $\bar{\eta} = -\eta^*$ and $\bar{L} = -L^*$).

Operator matrix $\boldsymbol{\mathcal{A}}$ in equations (1) and (2) obeys, for all wave phenomena of Table 1, the following symmetry properties

$$\boldsymbol{\mathcal{A}}^t\mathbf{N} = -\mathbf{N}\boldsymbol{\mathcal{A}}, \tag{7}$$
$$\boldsymbol{\mathcal{A}}^\dagger\mathbf{K} = -\mathbf{K}\bar{\boldsymbol{\mathcal{A}}}, \tag{8}$$
$$\boldsymbol{\mathcal{A}}^*\mathbf{J} = \mathbf{J}\bar{\boldsymbol{\mathcal{A}}}, \tag{9}$$

with

$$\mathbf{N} = \begin{pmatrix} \mathbf{O} & \mathbf{I} \\ -\mathbf{I} & \mathbf{O} \end{pmatrix}, \quad \mathbf{K} = \begin{pmatrix} \mathbf{O} & \mathbf{I} \\ \mathbf{I} & \mathbf{O} \end{pmatrix}, \quad \mathbf{J} = \begin{pmatrix} \mathbf{I} & \mathbf{O} \\ \mathbf{O} & -\mathbf{I} \end{pmatrix}, \tag{10}$$

where $\mathbf{I}$ is an identity matrix (here it is a $N/2 \times N/2$ matrix, but at other places it is a $N \times N$ matrix). Superscript t in equation (7) denotes transposition. In particular, it involves matrix transposition and transposition of the operators within the matrix. It should be noted that $\partial_\alpha^t = -\partial_\alpha$ for $\alpha = 1, 2$. Moreover, the transpose of a product of operators is equal to the product of the transposed operators in reverse order, for example $(\partial_1 \frac{1}{\mathcal{E}} \partial_2)^t = \partial_2^t \frac{1}{\mathcal{E}} \partial_1^t = \partial_2 \frac{1}{\mathcal{E}} \partial_1$. Superscript $\dagger$ in equation (8) denotes transposition and complex conjugation. Similar as superscript t, it applies to the matrix and to the operators within the matrix. The overbar in equations (8) and (9) means that the medium parameters (or potential) in the operator matrix are replaced by their adjoints. Note that symmetry relations (7) – (9) do not rely on $\mathcal{PT}$-symmetry.

Next, we consider $\mathcal{PT}$-symmetric materials. For all wave phenomena of Table 1 (except for seismoelectric waves, which will be treated separately), we call a medium $\mathcal{PT}$-symmetric when each parameter $m(\mathbf{x}, \omega)$ obeys the symmetry relation

$$m(-\mathbf{x}, \omega) = \bar{m}(\mathbf{x}, \omega). \tag{11}$$

The overbar denotes again the adjoint parameter which, as discussed above, is the complex conjugate (and in some cases minus the complex conjugate) of the original parameter. Since complex conjugation in the frequency domain corresponds to time-reversal in the time domain, equation (11) quantifies symmetry in space and time. With this relation, we find for all wave phenomena of Table 1 (except for seismoelectric waves) the following additional symmetry property of operator matrix $\boldsymbol{\mathcal{A}}$

$$\boldsymbol{\mathcal{A}}(-\mathbf{x}, \omega, -\partial_\alpha) = -\boldsymbol{\mathcal{A}}^*(\mathbf{x}, \omega, \partial_\alpha). \tag{12}$$

For seismoelectric waves we define for Onsager's coupling factor L the $\mathcal{PT}$-symmetry relation $L(-\mathbf{x}, \omega) = L^*(\mathbf{x}, \omega)$. This is different from equation (11), since we defined the adjoint of L earlier as $\bar{L} = -L^*$. Nevertheless, with this deviating $\mathcal{PT}$-symmetry relation for L (and all other parameters obeying equation (11)), symmetry relation (12) appears to hold also for the operator matrix $\boldsymbol{\mathcal{A}}$ for seismoelectric waves, defined in reference [41].

We obtain an auxiliary wave equation by replacing $\mathbf{x}$ by $-\mathbf{x}$, ∂_α by $-\partial_\alpha$ and ∂_3 by $-\partial_3$ in equation (1) and using symmetry relation (12). This gives

$$-\partial_3 \mathbf{q}(-\mathbf{x}, \omega) + \boldsymbol{\mathcal{A}}^*(\mathbf{x}, \omega, \partial_\alpha)\, \mathbf{q}(-\mathbf{x}, \omega) = \mathbf{d}(-\mathbf{x}, \omega). \tag{13}$$

In the following we drop the arguments ω and ∂_α for notational convenience.

3. Four reciprocity theorems

In this section we review two unified reciprocity theorems for arbitrary inhomogeneous media and we derive two new reciprocity theorems for $\mathcal{PT}$-symmetric media. Consider a spatial domain $\mathbb{D}$ with its center at the origin $\mathcal{O}$, enclosed by two infinite horizontal boundaries $\partial\mathbb{D}_-$ and $\partial\mathbb{D}_+$ at depth levels $x_3 = -x_{3,1}$ and $x_3 = x_{3,1}$, respectively,

Preprints (www.preprints.org) | NOT PEER-REVIEWED | Posted: 28 September 2022 doi:10.20944/preprints202209.0444.v1

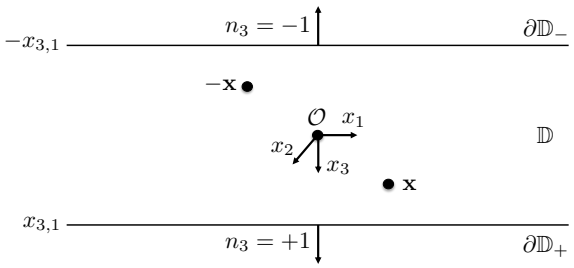

Figure 1. Configuration for the reciprocity theorems.

with outward pointing normal vectors $(0, 0, n_3 = -1)$ and $(0, 0, n_3 = +1)$, respectively, see Figure 1. We define $\partial\mathbb{D}$ as the union of the two boundaries, hence, $\partial\mathbb{D} = \partial\mathbb{D}_- \cup \partial\mathbb{D}_+$. In this configuration, we consider two independent wave states, where each state is characterised by a wave-field vector $\mathbf{q}$, a source vector $\mathbf{d}$ and an operator matrix $\boldsymbol{\mathcal{A}}$. We will distinguish the two states with subscripts A and B. Both states obey wave equation (1); when the medium in $\mathbb{D}$ is $\mathcal{PT}$-symmetric they also obey wave equation (13). We derive reciprocity theorems, which formulate relations between the wave states A and B [24–27,44–47]. For the configuration of Figure 1 we follow the approach of references [41,48,49].

Consider the quantity $\partial_3\{\mathbf{q}_A^t(\mathbf{x})\mathbf{N}\mathbf{q}_B(\mathbf{x})\}$. Applying the product rule for differentiation gives

$$\partial_3\{\mathbf{q}_A^t(\mathbf{x})\mathbf{N}\mathbf{q}_B(\mathbf{x})\} = \{\partial_3\mathbf{q}_A^t(\mathbf{x})\}\mathbf{N}\mathbf{q}_B(\mathbf{x}) + \mathbf{q}_A^t(\mathbf{x})\mathbf{N}\{\partial_3\mathbf{q}_B(\mathbf{x})\}. \tag{14}$$

Integrating both sides over domain $\mathbb{D}$, using the theorem of Gauss on the left-hand side and wave equation (1) on the right-hand side yields

$$\int_{\partial\mathbb{D}} \mathbf{q}_A^t(\mathbf{x})\mathbf{N}\mathbf{q}_B(\mathbf{x})n_3\mathrm{d}^2\mathbf{x}_\mathrm{H} = \int_{\mathbb{D}} \Big[\{\boldsymbol{\mathcal{A}}_A(\mathbf{x})\mathbf{q}_A(\mathbf{x}) + \mathbf{d}_A(\mathbf{x})\}^t\mathbf{N}\mathbf{q}_B(\mathbf{x}) + \mathbf{q}_A^t(\mathbf{x})\mathbf{N}\{\boldsymbol{\mathcal{A}}_B(\mathbf{x})\mathbf{q}_B(\mathbf{x}) + \mathbf{d}_B(\mathbf{x})\}\Big]\mathrm{d}^3\mathbf{x}. \tag{15}$$

Here $\mathbf{x}_\mathrm{H}$ is the horizontal coordinate vector (x_1, x_2). Using symmetry relation (7) on the right-hand side and reordering the terms gives

$$\int_{\partial\mathbb{D}} \mathbf{q}_A^t(\mathbf{x})\mathbf{N}\mathbf{q}_B(\mathbf{x})n_3\mathrm{d}^2\mathbf{x}_\mathrm{H} = \int_{\mathbb{D}} \Big[\mathbf{q}_A^t(\mathbf{x})\mathbf{N}\{\boldsymbol{\mathcal{A}}_B(\mathbf{x}) - \boldsymbol{\mathcal{A}}_A(\mathbf{x})\}\mathbf{q}_B(\mathbf{x}) + \mathbf{d}_A^t(\mathbf{x})\mathbf{N}\mathbf{q}_B(\mathbf{x}) + \mathbf{q}_A^t(\mathbf{x})\mathbf{N}\mathbf{d}_B(\mathbf{x})\Big]\mathrm{d}^3\mathbf{x}. \tag{16}$$

This is a unified reciprocity theorem of the convolution type (since terms like $\mathbf{q}_A^t(\mathbf{x})\mathbf{N}\mathbf{q}_B(\mathbf{x})$ in the frequency domain correspond to convolutions in the time domain). It does not rely on $\mathcal{PT}$-symmetry.

Next, consider the quantity $\partial_3\{\mathbf{q}_A^\dagger(-\mathbf{x})\mathbf{N}\mathbf{q}_B(\mathbf{x})\}$. Following a similar procedure as above, but this time using auxiliary wave equation (13), we obtain

$$\int_{\partial\mathbb{D}} \mathbf{q}_A^\dagger(-\mathbf{x})\mathbf{N}\mathbf{q}_B(\mathbf{x})n_3\mathrm{d}^2\mathbf{x}_\mathrm{H} = \int_{\mathbb{D}} \Big[\mathbf{q}_A^\dagger(-\mathbf{x})\mathbf{N}\{\boldsymbol{\mathcal{A}}_B(\mathbf{x}) - \boldsymbol{\mathcal{A}}_A(\mathbf{x})\}\mathbf{q}_B(\mathbf{x}) - \mathbf{d}_A^\dagger(-\mathbf{x})\mathbf{N}\mathbf{q}_B(\mathbf{x}) + \mathbf{q}_A^\dagger(-\mathbf{x})\mathbf{N}\mathbf{d}_B(\mathbf{x})\Big]\mathrm{d}^3\mathbf{x}. \tag{17}$$

This is a unified reciprocity theorem of the correlation type (since terms like $\mathbf{q}_A^\dagger(-\mathbf{x})\mathbf{N}\mathbf{q}_B(\mathbf{x})$ in the frequency domain correspond to correlations in the time domain). Since we used wave equation (13) for its derivation, it only holds for $\mathcal{PT}$-symmetric media. Note that the integration boundary on the left-hand side is defined as $\partial\mathbb{D} = \partial\mathbb{D}_- \cup \partial\mathbb{D}_+$. For the integration along $\partial\mathbb{D}_-$, the fields $\mathbf{q}_A(-\mathbf{x})$ and $\mathbf{q}_B(\mathbf{x})$ are evaluated at $\partial\mathbb{D}_+$ and $\partial\mathbb{D}_-$, respectively. Similarly, for the integration along $\partial\mathbb{D}_+$, the fields $\mathbf{q}_A(-\mathbf{x})$ and $\mathbf{q}_B(\mathbf{x})$ are evaluated at $\partial\mathbb{D}_-$ and $\partial\mathbb{D}_+$, respectively.

Preprints (www.preprints.org) | NOT PEER-REVIEWED | Posted: 28 September 2022 doi:10.20944/preprints202209.0444.v1

Next, consider the quantity $\partial_3\{\mathbf{q}_A^\dagger(\mathbf{x})\mathbf{K}\mathbf{q}_B(\mathbf{x})\}$. A similar procedure as above, using wave equation (1) and symmetry relation (8), yields

$$\int_{\partial\mathbb{D}} \mathbf{q}_A^\dagger(\mathbf{x})\mathbf{K}\mathbf{q}_B(\mathbf{x})n_3\mathrm{d}^2\mathbf{x}_\mathrm{H} = \int_{\mathbb{D}} \Big[\mathbf{q}_A^\dagger(\mathbf{x})\mathbf{K}\{\boldsymbol{\mathcal{A}}_B(\mathbf{x}) - \bar{\boldsymbol{\mathcal{A}}}_A(\mathbf{x})\}\mathbf{q}_B(\mathbf{x}) + \mathbf{d}_A^\dagger(\mathbf{x})\mathbf{K}\mathbf{q}_B(\mathbf{x}) + \mathbf{q}_A^\dagger(\mathbf{x})\mathbf{K}\mathbf{d}_B(\mathbf{x})\Big]\mathrm{d}^3\mathbf{x}. \tag{18}$$

This is a unified reciprocity theorem of the correlation type which does not rely on $\mathcal{PT}$-symmetry.

Finally, consider the quantity $\partial_3\{\mathbf{q}_A^t(-\mathbf{x})\mathbf{K}\mathbf{q}_B(\mathbf{x})\}$. Following the same procedure, using auxiliary wave equation (13) and symmetry relation (8), yields

$$\int_{\partial\mathbb{D}} \mathbf{q}_A^t(-\mathbf{x})\mathbf{K}\mathbf{q}_B(\mathbf{x})n_3\mathrm{d}^2\mathbf{x}_\mathrm{H} = \int_{\mathbb{D}} \Big[\mathbf{q}_A^t(-\mathbf{x})\mathbf{K}\{\boldsymbol{\mathcal{A}}_B(\mathbf{x}) - \bar{\boldsymbol{\mathcal{A}}}_A(\mathbf{x})\}\mathbf{q}_B(\mathbf{x}) - \mathbf{d}_A^t(-\mathbf{x})\mathbf{K}\mathbf{q}_B(\mathbf{x}) + \mathbf{q}_A^t(-\mathbf{x})\mathbf{K}\mathbf{d}_B(\mathbf{x})\Big]\mathrm{d}^3\mathbf{x}. \tag{19}$$

This is a unified reciprocity theorem of the convolution type which only holds for $\mathcal{PT}$-symmetric media.

Equations (16) and (18) were already known [41,48,49]; they hold for arbitrary inhomogeneous media. Equations (17) and (19) are new; they hold for inhomogeneous media media with $\mathcal{PT}$ symmetry. We will use these reciprocity theorems as a basis to derive unified wave field representations (section 5), relations between reflection and transmission responses (section 6), and a Marchenko scheme (section 7). Before we come to this, we first analyze the boundary integrals in the four reciprocity theorems.

4. Analysis of the boundary integrals

For the analysis of the boundary integrals we define a $N \times 1$ wave-field vector $\mathbf{p}$, according to

$$\mathbf{p} = \begin{pmatrix} \mathbf{p}^+ \\ \mathbf{p}^- \end{pmatrix}, \tag{20}$$

where $\mathbf{p}^+$ and $\mathbf{p}^-$ are $N/2 \times 1$ vectors containing flux-normalised downgoing and upgoing wave fields, respectively (for a comprehensive discussion on flux-normalised versus field-normalised decomposition, see reference [50]). At the boundary $\partial\mathbb{D}$ we relate the wave-field vector $\mathbf{q}$ to $\mathbf{p}$ in states A and B via

$$\mathbf{q}_A(\mathbf{x}) = \boldsymbol{\mathcal{L}}(\mathbf{x})\mathbf{p}_A(\mathbf{x}), \tag{21}$$
$$\mathbf{q}_B(\mathbf{x}) = \boldsymbol{\mathcal{L}}(\mathbf{x})\mathbf{p}_B(\mathbf{x}), \tag{22}$$

for $x_3 = \pm x_{3,1}$, where $\boldsymbol{\mathcal{L}}(\mathbf{x})$ is a $N \times N$ operator matrix, which composes the wave-field vectors $\mathbf{q}_{A,B}$ from their downgoing and upgoing constituents $\mathbf{p}_{A,B}^+$ and $\mathbf{p}_{A,B}^-$. Note that $\boldsymbol{\mathcal{L}}$ in equations (21) and (22) is without subscript A or B, which implies that we assume that the medium parameters (or potentials) at $\partial\mathbb{D}$ in both states are identical. Explicit expressions for the spatial Fourier transform of $\boldsymbol{\mathcal{L}}$, assuming the medium parameters (or potential) at $\partial\mathbb{D}$ are laterally invariant, are given in Appendix A for acoustic, quantum-mechanical, electromagnetic and elastodynamic waves. Substituting equations (21) and (22) in the boundary integrals of reciprocity theorems (16) and (17), we derive in Appendix B, using specific symmetry properties of $\boldsymbol{\mathcal{L}}$,

$$\int_{\partial\mathbb{D}} \mathbf{q}_A^t(\mathbf{x})\mathbf{N}\mathbf{q}_B(\mathbf{x})n_3\mathrm{d}^2\mathbf{x}_\mathrm{H} = -\int_{\partial\mathbb{D}} \mathbf{p}_A^t(\mathbf{x})\mathbf{N}\mathbf{p}_B(\mathbf{x})n_3\mathrm{d}^2\mathbf{x}_\mathrm{H}, \tag{23}$$
$$\int_{\partial\mathbb{D}} \mathbf{q}_A^\dagger(-\mathbf{x})\mathbf{N}\mathbf{q}_B(\mathbf{x})n_3\mathrm{d}^2\mathbf{x}_\mathrm{H} = -\int_{\partial\mathbb{D}} \mathbf{p}_A^\dagger(-\mathbf{x})\mathbf{N}\mathbf{p}_B(\mathbf{x})n_3\mathrm{d}^2\mathbf{x}_\mathrm{H}. \tag{24}$$

Preprints (www.preprints.org) | NOT PEER-REVIEWED | Posted: 28 September 2022 doi:10.20944/preprints202209.0444.v1

For the analysis of the boundary integrals of reciprocity theorems (18) and (19), we first replace equation (21) by

$$\mathbf{q}_A(\mathbf{x}) \;=\; \bar{\boldsymbol{\mathcal{L}}}(\mathbf{x})\mathbf{p}_A(\mathbf{x}), \tag{25}$$

for $x_3 = \pm x_{3,1}$, where operator matrix $\bar{\boldsymbol{\mathcal{L}}}$ is defined in the adjoint medium at $\partial\mathbb{D}$. Substituting equations (22) and (25) in the boundary integrals of reciprocity theorems (18) and (19), we derive in Appendix B, using specific symmetry properties of $\bar{\boldsymbol{\mathcal{L}}}$,

$$\int_{\partial\mathbb{D}} \mathbf{q}_A^\dagger(\mathbf{x})\mathbf{K}\mathbf{q}_B(\mathbf{x})n_3\mathrm{d}^2\mathbf{x}_\mathrm{H} \;=\; \int_{\partial\mathbb{D}} \mathbf{p}_A^\dagger(\mathbf{x})\mathbf{J}\mathbf{p}_B(\mathbf{x})n_3\mathrm{d}^2\mathbf{x}_\mathrm{H}, \tag{26}$$

$$\int_{\partial\mathbb{D}} \mathbf{q}_A^t(-\mathbf{x})\mathbf{K}\mathbf{q}_B(\mathbf{x})n_3\mathrm{d}^2\mathbf{x}_\mathrm{H} \;=\; \int_{\partial\mathbb{D}} \mathbf{p}_A^t(-\mathbf{x})\mathbf{J}\mathbf{p}_B(\mathbf{x})n_3\mathrm{d}^2\mathbf{x}_\mathrm{H}. \tag{27}$$

Equations (23) and (26) were already known [51]. Equations (24) and (27) are new; they only hold for boundaries with $\mathcal{PT}$ symmetry. For equations (23) and (24) we assumed that the medium at $\partial\mathbb{D}$ in state A is the same as that in state B, whereas for equations (26) and (27) we assumed that the medium at $\partial\mathbb{D}$ in state A is the adjoint of that in state B. For all four equations we assumed that the medium parameters at the boundary $\partial\mathbb{D}$ are laterally invariant; the medium parameters in $\mathbb{D}$ can still be laterally varing.

Using equations (10) and (20), we can rewrite the right-hand sides of equations (23) (24), (26) and (27) explicitly in terms of downgoing and upgoing waves at $\partial\mathbb{D}$, according to

$$\int_{\partial\mathbb{D}} \mathbf{q}_A^t(\mathbf{x})\mathbf{N}\mathbf{q}_B(\mathbf{x})n_3\mathrm{d}^2\mathbf{x}_\mathrm{H} \;=\; -\int_{\partial\mathbb{D}} \Big(\{\mathbf{p}_A^+(\mathbf{x})\}^t\mathbf{p}_B^-(\mathbf{x}) - \{\mathbf{p}_A^-(\mathbf{x})\}^t\mathbf{p}_B^+(\mathbf{x})\Big)n_3\mathrm{d}^2\mathbf{x}_\mathrm{H}, \tag{28}$$

$$\int_{\partial\mathbb{D}} \mathbf{q}_A^\dagger(-\mathbf{x})\mathbf{N}\mathbf{q}_B(\mathbf{x})n_3\mathrm{d}^2\mathbf{x}_\mathrm{H} \;=\; -\int_{\partial\mathbb{D}} \Big(\{\mathbf{p}_A^+(-\mathbf{x})\}^\dagger\mathbf{p}_B^-(\mathbf{x}) - \{\mathbf{p}_A^-(-\mathbf{x})\}^\dagger\mathbf{p}_B^+(\mathbf{x})\Big)n_3\mathrm{d}^2\mathbf{x}_\mathrm{H}, \tag{29}$$

$$\int_{\partial\mathbb{D}} \mathbf{q}_A^\dagger(\mathbf{x})\mathbf{K}\mathbf{q}_B(\mathbf{x})n_3\mathrm{d}^2\mathbf{x}_\mathrm{H} \;=\; \int_{\partial\mathbb{D}} \Big(\{\mathbf{p}_A^+(\mathbf{x})\}^\dagger\mathbf{p}_B^+(\mathbf{x}) - \{\mathbf{p}_A^-(\mathbf{x})\}^\dagger\mathbf{p}_B^-(\mathbf{x})\Big)n_3\mathrm{d}^2\mathbf{x}_\mathrm{H}, \tag{30}$$

$$\int_{\partial\mathbb{D}} \mathbf{q}_A^t(-\mathbf{x})\mathbf{K}\mathbf{q}_B(\mathbf{x})n_3\mathrm{d}^2\mathbf{x}_\mathrm{H} \;=\; \int_{\partial\mathbb{D}} \Big(\{\mathbf{p}_A^+(-\mathbf{x})\}^t\mathbf{p}_B^+(\mathbf{x}) - \{\mathbf{p}_A^-(-\mathbf{x})\}^t\mathbf{p}_B^-(\mathbf{x})\Big)n_3\mathrm{d}^2\mathbf{x}_\mathrm{H}. \tag{31}$$

Equations (29) and (31) only hold for boundaries with $\mathcal{PT}$ symmetry. For equations (28) and (29) we assumed that the medium at $\partial\mathbb{D}$ in state A is the same as that in state B, whereas for equations (30) and (31) we assumed that the medium at $\partial\mathbb{D}$ in state A is the adjoint of that in state B.

These equations will be used in section 6 for the derivation of relations between reflection and transmission responses. Here we consider a special case. Let us assume that the medium outside $\mathbb{D}$ is homogeneous and source free and that the wave fields in both states are responses to sources in $\mathbb{D}$. This implies that at $\partial\mathbb{D}$ all waves are outward propagating, i.e., at $\partial\mathbb{D}_-$ there are only upgoing waves and at $\partial\mathbb{D}_+$ only downgoing waves. Hence, $\mathbf{p}_A^+(\mathbf{x}) = \mathbf{p}_B^+(\mathbf{x}) = \mathbf{p}_A^-(-\mathbf{x}) = \mathbf{p}_B^-(-\mathbf{x}) = \mathbf{0}$ for $\mathbf{x}$ at $\partial\mathbb{D}_-$ and $\mathbf{p}_A^+(-\mathbf{x}) = \mathbf{p}_B^+(-\mathbf{x}) = \mathbf{p}_A^-(\mathbf{x}) = \mathbf{p}_B^-(\mathbf{x}) = \mathbf{0}$ for $\mathbf{x}$ at $\partial\mathbb{D}_+$ (here $\mathbf{0}$ is a $N/2 \times 1$ zero vector). Using this in equations (28) and (31) yields

$$\int_{\partial\mathbb{D}} \mathbf{q}_A^t(\mathbf{x})\mathbf{N}\mathbf{q}_B(\mathbf{x})n_3\mathrm{d}^2\mathbf{x}_\mathrm{H} \;=\; 0, \tag{32}$$

$$\int_{\partial\mathbb{D}} \mathbf{q}_A^t(-\mathbf{x})\mathbf{K}\mathbf{q}_B(\mathbf{x})n_3\mathrm{d}^2\mathbf{x}_\mathrm{H} \;=\; 0. \tag{33}$$

Equation (32) is the well-known Sommerfeld radiation condition; it holds under the condition that the medium at $\partial\mathbb{D}$ in state A is the same as that in state B. Equation (33) is a new radiation condition; it only holds for boundaries with $\mathcal{PT}$ symmetry under the condition that the medium at $\partial\mathbb{D}$ in state A is the adjoint of that in state B.

Preprints (www.preprints.org) | NOT PEER-REVIEWED | Posted: 28 September 2022 doi:10.20944/preprints202209.0444.v1

5. Wave field representations

We use the reciprocity theorems derived in section 3 as the basis for deriving wave field representations. In section 5.1 we discuss the unified Green's matrix and its symmetry properties. In section 5.2 we derive a wave field representation by choosing the Green's state for state A. In section 5.3 we derive representations for back-propagation and for Green's matrix retrieval, also known as interferometry. We consider arbitrary inhomogeneous media and media with $\mathcal{PT}$-symmetry.

5.1. The Green's matrix and its symmetry properties

We introduce the $N \times N$ Green's matrix $\mathbf{G}(\mathbf{x}, \mathbf{x}_A)$ for an arbitrary inhomogeneous medium as the solution of

$$\partial_3 \mathbf{G} - \boldsymbol{\mathcal{A}}\mathbf{G} = \mathbf{I}\delta(\mathbf{x} - \mathbf{x}_A), \tag{34}$$

where $\mathbf{x}_A = (x_{1,A}, x_{2,A}, x_{3,A})$ defines the position of a unit point source. We further demand that the time-domain Green's matrix $\mathbf{G}(\mathbf{x}, \mathbf{x}_A, t)$ is causal, hence $\mathbf{G}(\mathbf{x}, \mathbf{x}_A, t < 0) = \mathbf{O}$. Similar to operator matrix $\boldsymbol{\mathcal{A}}$, the Green's matrix is partitioned as

$$\mathbf{G}(\mathbf{x}, \mathbf{x}_A) = \begin{pmatrix} \mathbf{G}_{11} & \mathbf{G}_{12} \\ \mathbf{G}_{21} & \mathbf{G}_{22} \end{pmatrix} (\mathbf{x}, \mathbf{x}_A). \tag{35}$$

We derive a symmetry property of the Green's matrix. We replace $\mathbf{q}_A$ and $\mathbf{q}_B$ in reciprocity theorem (16) by Green's matrices $\mathbf{G}(\mathbf{x}, \mathbf{x}_A)$ and $\mathbf{G}(\mathbf{x}, \mathbf{x}_B)$, respectively. Similarly, we replace the source vectors $\mathbf{d}_A$ and $\mathbf{d}_B$ by $\mathbf{I}\delta(\mathbf{x} - \mathbf{x}_A)$ and $\mathbf{I}\delta(\mathbf{x} - \mathbf{x}_B)$, respectively, with $\mathbf{x}_A$ and $\mathbf{x}_B$ denoting the source positions, both in $\mathbb{D}$. Both Green's matrices are defined in the same medium, hence, $\boldsymbol{\mathcal{A}}_A = \boldsymbol{\mathcal{A}}_B = \boldsymbol{\mathcal{A}}$. This implies that the first term under the integral on the right-hand side of equation (16) vanishes. We assume the medium outside $\mathbb{D}$ is homogeneous, so that the Green's matrices at $\partial\mathbb{D}$ are outward propagating. This implies that the integral on the left-hand side of equation (16) also vanishes, see equation (32). From the remaining integral we thus obtain the following symmetry property of the Green's matrix

$$\mathbf{G}^t(\mathbf{x}_B, \mathbf{x}_A)\mathbf{N} = -\mathbf{N}\mathbf{G}(\mathbf{x}_A, \mathbf{x}_B). \tag{36}$$

This is the well-known source-receiver reciprocity relation, which holds for arbitrary inhomogeneous media. It is illustrated in Figure 2(a). Next, we define $\bar{\mathbf{G}}(\mathbf{x}, \mathbf{x}_A)$ as the outward propagating Green's matrix of the adjoint medium, obeying the following wave equation

$$\partial_3 \bar{\mathbf{G}} - \bar{\boldsymbol{\mathcal{A}}}\bar{\mathbf{G}} = \mathbf{I}\delta(\mathbf{x} - \mathbf{x}_A). \tag{37}$$

We will combine $\mathbf{G}(\mathbf{x}, \mathbf{x}_A)$ and the complex conjugate of $\bar{\mathbf{G}}(\mathbf{x}, \mathbf{x}_A)$ to form a so-called homogeneous Green's matrix, i.e., a Green's matrix obeying a wave equation without a source term on the right-hand side. To this end, we first pre-and post-multiply all terms in equation (37) by $\mathbf{J}$, use equation (9) and $\mathbf{JJ} = \mathbf{I}$ and subsequently take the complex conjugate of all terms. This yields

$$\partial_3 \mathbf{J}\bar{\mathbf{G}}^*\mathbf{J} - \boldsymbol{\mathcal{A}}\mathbf{J}\bar{\mathbf{G}}^*\mathbf{J} = \mathbf{I}\delta(\mathbf{x} - \mathbf{x}_A). \tag{38}$$

Subtracting all terms of this equation from the corresponding terms in equation (34) yields

$$\partial_3 \mathbf{G}_\mathrm{h} - \boldsymbol{\mathcal{A}}\mathbf{G}_\mathrm{h} = \mathbf{O} \tag{39}$$

with the homogeneous Green's matrix $\mathbf{G}_\mathrm{h}(\mathbf{x}, \mathbf{x}_A)$ defined as

$$\mathbf{G}_\mathrm{h}(\mathbf{x}, \mathbf{x}_A) = \mathbf{G}(\mathbf{x}, \mathbf{x}_A) - \mathbf{J}\bar{\mathbf{G}}^*(\mathbf{x}, \mathbf{x}_A)\mathbf{J}. \tag{40}$$

Preprints (www.preprints.org) | NOT PEER-REVIEWED | Posted: 28 September 2022 doi:10.20944/preprints202209.0444.v1

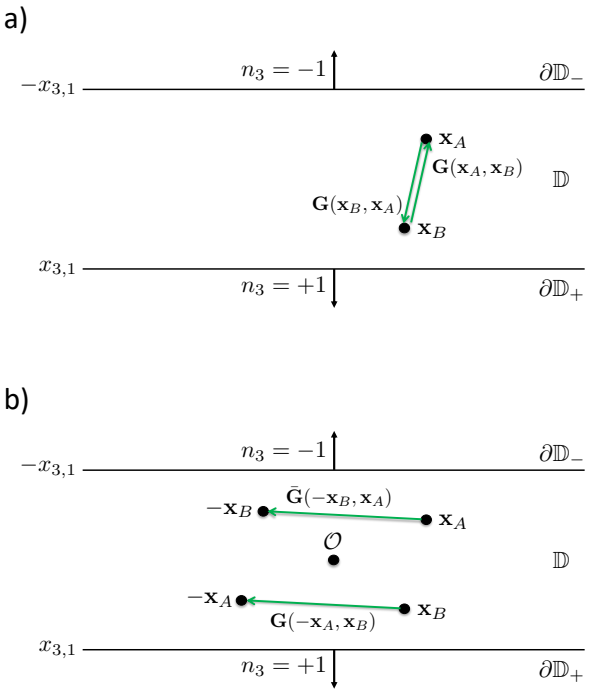

Figure 2. (a) Source-receiver reciprocity for an arbitrary inhomogeneous medium (equations (36) and (41)). (b) Additional source-receiver reciprocity for a medium with $\mathcal{PT}$-symmetry (equations (42) and (43)). The rays in these and subsequent figures represent full multi-component responses (direct waves, (multiply-)scattered waves, converted waves etc.) between the source and receiver points.

Using symmetry relation (36), $\mathbf{JN} = -\mathbf{NJ}$ and $\mathbf{J}^t = \mathbf{J}$, we find the following reciprocity relation for the homogeneous Green's matrix

$$\mathbf{G}_{\mathrm{h}}^t(\mathbf{x}_B, \mathbf{x}_A)\mathbf{N} = -\mathbf{N}\mathbf{G}_{\mathrm{h}}(\mathbf{x}_A, \mathbf{x}_B). \tag{41}$$

Next, we derive symmetry properties of the Green's matrix and the homogeneous Green's matrix for $\mathcal{PT}$-symmetric media. We replace $\mathbf{q}_A$ and $\mathbf{q}_B$ in reciprocity theorem (19) by Green's matrices $\bar{\mathbf{G}}(\mathbf{x}, \mathbf{x}_A)$ and $\mathbf{G}(\mathbf{x}, \mathbf{x}_B)$, respectively. Since $\boldsymbol{\mathcal{A}}_A = \bar{\boldsymbol{\mathcal{A}}}$ (see equation (37)) and $\boldsymbol{\mathcal{A}}_B = \boldsymbol{\mathcal{A}}$ (as before) we have $\bar{\boldsymbol{\mathcal{A}}}_A = \boldsymbol{\mathcal{A}}_B$, hence, the first term under the integral on the right-hand side of equation (19) vanishes. Assuming the medium outside $\mathbb{D}$ is homogeneous, the integral on the left-hand side of equation (19) also vanishes, see equation (33). From the remaining integral we thus obtain the following symmetry property of the Green's matrix

$$\bar{\mathbf{G}}^t(-\mathbf{x}_B, \mathbf{x}_A)\mathbf{K} = \mathbf{K}\mathbf{G}(-\mathbf{x}_A, \mathbf{x}_B). \tag{42}$$

This is an additional source-receiver reciprocity relation, which only holds for media with $\mathcal{PT}$-symmetry. It is illustrated in Figure 2(b). Using symmetry relation (42), $\mathbf{JK} = -\mathbf{KJ}$ and $\mathbf{J}^t = \mathbf{J}$, we find the following reciprocity relation for the homogeneous Green's matrix in $\mathcal{PT}$-symmetric media

$$\bar{\mathbf{G}}_{\mathrm{h}}^t(-\mathbf{x}_B, \mathbf{x}_A)\mathbf{K} = \mathbf{K}\mathbf{G}_{\mathrm{h}}(-\mathbf{x}_A, \mathbf{x}_B). \tag{43}$$

5.2. Wave field representation

We derive a general wave field representation from the reciprocity theorem of the convolution type for arbitrary inhomogeneous media (equation (16)). For state A we choose the Green's state, hence, we replace $\mathbf{q}_A$ and $\mathbf{d}_A$ by Green's matrix $\mathbf{G}(\mathbf{x}, \mathbf{x}_A)$ and unit source

Preprints (www.preprints.org) | NOT PEER-REVIEWED | Posted: 28 September 2022 doi:10.20944/preprints202209.0444.v1

matrix $\mathbf{I}\delta(\mathbf{x}-\mathbf{x}_A)$; we leave operator $\boldsymbol{\mathcal{A}}_A$ as is. For state B we choose the actual wave state. To this end we drop the subscripts B from $\mathbf{q}_B$, $\mathbf{d}_B$ and $\boldsymbol{\mathcal{A}}_B$. We thus obtain from equation (16)

$$\chi_{\mathbb{D}}(\mathbf{x}_A)\mathbf{N}\mathbf{q}(\mathbf{x}_A) = -\int_{\mathbb{D}} \mathbf{G}^t(\mathbf{x},\mathbf{x}_A)\mathbf{N}\mathbf{d}(\mathbf{x})\mathrm{d}^3\mathbf{x} + \int_{\partial\mathbb{D}} \mathbf{G}^t(\mathbf{x},\mathbf{x}_A)\mathbf{N}\mathbf{q}(\mathbf{x})n_3\mathrm{d}^2\mathbf{x}_{\mathrm{H}} - \int_{\mathbb{D}} \mathbf{G}^t(\mathbf{x},\mathbf{x}_A)\mathbf{N}\{\boldsymbol{\mathcal{A}}-\boldsymbol{\mathcal{A}}_A\}\mathbf{q}(\mathbf{x})\mathrm{d}^3\mathbf{x}, \quad (44)$$

where $\chi_{\mathbb{D}}(\mathbf{x})$ is the characteristic function for domain $\mathbb{D}$, defined as

$$\chi_{\mathbb{D}}(\mathbf{x}) = \begin{cases} 1, & \text{for } \mathbf{x} \text{ inside } \mathbb{D}, \\ \frac{1}{2}, & \text{for } \mathbf{x} \text{ on } \partial\mathbb{D}, \\ 0, & \text{for } \mathbf{x} \text{ outside } \mathbb{D}. \end{cases} \quad (45)$$

Using the symmetry property of the Green's matrix, formulated by equation (36), we obtain

$$\chi_{\mathbb{D}}(\mathbf{x}_A)\mathbf{q}(\mathbf{x}_A) = \int_{\mathbb{D}} \mathbf{G}(\mathbf{x}_A,\mathbf{x})\mathbf{d}(\mathbf{x})\mathrm{d}^3\mathbf{x} - \int_{\partial\mathbb{D}} \mathbf{G}(\mathbf{x}_A,\mathbf{x})\mathbf{q}(\mathbf{x})n_3\mathrm{d}^2\mathbf{x}_{\mathrm{H}} + \int_{\mathbb{D}} \mathbf{G}(\mathbf{x}_A,\mathbf{x})\{\boldsymbol{\mathcal{A}}-\boldsymbol{\mathcal{A}}_A\}\mathbf{q}(\mathbf{x})\mathrm{d}^3\mathbf{x}. \quad (46)$$

This is the unified wave field representation of the convolution type, which does not rely on $\mathcal{PT}$-symmetry. The left-hand side is the wave field vector $\mathbf{q}(\mathbf{x}_A)$ at a specific position $\mathbf{x}_A$. It is expressed in terms of a volume integral containing the source distribution $\mathbf{d}(\mathbf{x})$ in $\mathbb{D}$, a unified Kirchhoff-Helmholtz boundary integral and an integral containing the contrast operator $\boldsymbol{\mathcal{A}}-\boldsymbol{\mathcal{A}}_A$ in $\mathbb{D}$. It finds applications in forward modelling [48,49,52], of which a further discussion is beyond the scope of this paper.

5.3. Back-propagation and interferometric Green's matrix retrieval

We derive representations for back-propagation and for interferometric Green's matrix retrieval from the reciprocity theorem of the correlation type for arbitrary inhomogeneous media (equation (18)). We replace the wave-field vectors $\mathbf{q}_A$ and $\mathbf{q}_B$ by Green's matrices $\bar{\mathbf{G}}(\mathbf{x},\mathbf{x}_A)$ and $\mathbf{G}(\mathbf{x},\mathbf{x}_B)$, respectively. Accordingly, the source vectors $\mathbf{d}_A$ and $\mathbf{d}_B$ are replaced by source matrices $\mathbf{I}\delta(\mathbf{x}-\mathbf{x}_A)$ and $\mathbf{I}\delta(\mathbf{x}-\mathbf{x}_B)$. For the operator matrices we choose $\boldsymbol{\mathcal{A}}_A = \bar{\boldsymbol{\mathcal{A}}}$ (since the Green's matrix in state A is defined in the adjoint medium) and $\boldsymbol{\mathcal{A}}_B = \boldsymbol{\mathcal{A}}$. These choices imply that the first term under the integral on the right-hand side of equation (18) vanishes. From the remaining terms in this equation we obtain

$$\chi_{\mathbb{D}}(\mathbf{x}_A)\mathbf{K}\mathbf{G}(\mathbf{x}_A,\mathbf{x}_B) + \chi_{\mathbb{D}}(\mathbf{x}_B)\bar{\mathbf{G}}^{\dagger}(\mathbf{x}_B,\mathbf{x}_A)\mathbf{K} = \int_{\partial\mathbb{D}} \bar{\mathbf{G}}^{\dagger}(\mathbf{x},\mathbf{x}_A)\mathbf{K}\mathbf{G}(\mathbf{x},\mathbf{x}_B)n_3\mathrm{d}^2\mathbf{x}_{\mathrm{H}}. \quad (47)$$

Next, we take both $\mathbf{x}_A$ and $\mathbf{x}_B$ in $\mathbb{D}$, hence, we can remove the characteristic functions from the left-hand side. Using $\mathbf{K} = -\mathbf{N}\mathbf{J}$, the symmetry property of the Green's matrix formulated by equation (36) and $\mathbf{N} = -\mathbf{K}\mathbf{J}$, we rewrite the second term on the left-hand side as $-\mathbf{K}\mathbf{J}\bar{\mathbf{G}}^{*}(\mathbf{x}_A,\mathbf{x}_B)\mathbf{J}$. Pre-multiplying both sides of the resulting equation by $\mathbf{K}^{-1}$ and using $\mathbf{K}^{-1} = \mathbf{K}$, we thus obtain

$$\mathbf{G}_{\mathrm{h}}(\mathbf{x}_A,\mathbf{x}_B) = \int_{\partial\mathbb{D}} \mathbf{K}\bar{\mathbf{G}}^{\dagger}(\mathbf{x},\mathbf{x}_A)\mathbf{K}\mathbf{G}(\mathbf{x},\mathbf{x}_B)n_3\mathrm{d}^2\mathbf{x}_{\mathrm{H}}, \quad (48)$$

with the homogeneous Green's matrix $\mathbf{G}_{\mathrm{h}}(\mathbf{x}_A,\mathbf{x}_B)$ defined in equation (40). Equation (48) is a unified form of the classical homogeneous Green's function representation [53,54]; it does not rely on $\mathcal{PT}$-symmetry. Equation (48) is illustrated in Figure 3(a). We can interpret $\mathbf{G}(\mathbf{x},\mathbf{x}_B)$ as the response to a source at $\mathbf{x}_B$ inside $\mathbb{D}$, observed by receivers at $\mathbf{x}$ at the boundary $\partial\mathbb{D}$, which consists of two planar boundaries $\partial\mathbb{D}_-$ and $\partial\mathbb{D}_+$. The Green's matrix $\bar{\mathbf{G}}^{\dagger}(\mathbf{x},\mathbf{x}_A)$ propagates this response back from $\mathbf{x}$ at the boundary to $\mathbf{x}_A$ inside $\mathbb{D}$. The result is the homogeneous Green's matrix between $\mathbf{x}_B$ and $\mathbf{x}_A$ (the red arrow in Figure 3(a)). When these two points coincide, then $\mathbf{G}_{\mathrm{h}}(\mathbf{x}_B,\mathbf{x}_B)$ can be interpreted as an image of the source at $\mathbf{x}_B$, obtained from observations at $\partial\mathbb{D}$. Equation (48) finds applications in (generalized forms

Preprints (www.preprints.org) | NOT PEER-REVIEWED | Posted: 28 September 2022 doi:10.20944/preprints202209.0444.v1

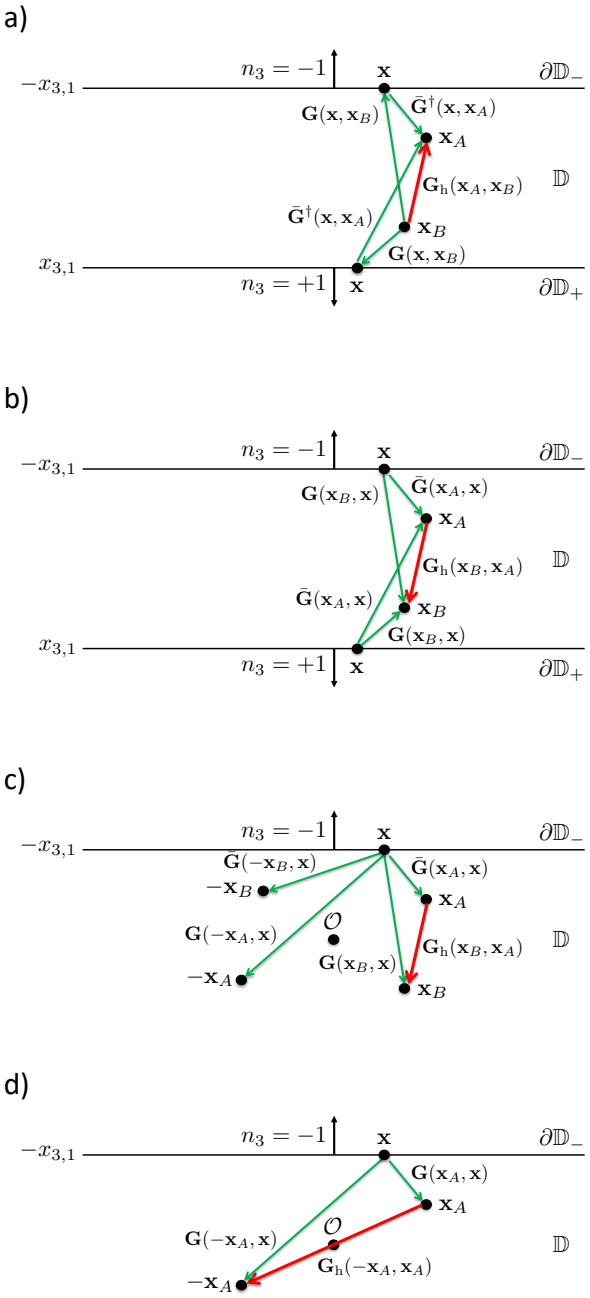

Figure 3. (a) Back propagation in an arbitrary inhomogeneous medium (equation 48). (b) Interferometric Green's matrix retrieval in an arbitrary inhomogeneous medium (equation 49). (c) Green's matrix retrieval in a medium with $\mathcal{PT}$-symmetry (equation 52). The integral is single-sided, but four receivers are required in the medium and its adjoint. (d) As in (c), but requiring two receivers only in one-and-the-same lossless medium (equation 53).

Preprints (www.preprints.org) | NOT PEER-REVIEWED | Posted: 28 September 2022 doi:10.20944/preprints202209.0444.v1

of) inverse source problems [46,55], inverse scattering [12,54,56,57], (holographic) imaging [53,58–62], time-reversal acoustics [63] and interferometric Green's matrix retrieval from passive measurements [64–66]. To explain the latter type of application, we transpose both sides of equation (48), use equations (36) and (41), $\mathbf{K} = \mathbf{K}^t$, $\mathbf{N}^{-1} = -\mathbf{N}$ and $\mathbf{NK} = -\mathbf{KN}$, to obtain

$$\mathbf{G}_\mathrm{h}(\mathbf{x}_B, \mathbf{x}_A) = -\int_{\partial\mathbb{D}} \mathbf{G}(\mathbf{x}_B, \mathbf{x})\mathbf{K}\bar{\mathbf{G}}^\dagger(\mathbf{x}_A, \mathbf{x})\mathbf{K}n_3 \mathrm{d}^2\mathbf{x}_\mathrm{H}. \tag{49}$$

When the medium is lossless, $\bar{\mathbf{G}}(\mathbf{x}_A, \mathbf{x})$ and $\mathbf{G}(\mathbf{x}_B, \mathbf{x})$ can be interpreted as responses to sources at $\mathbf{x}$ at the boundary $\partial\mathbb{D}$, observed by receivers at $\mathbf{x}_A$ and $\mathbf{x}_B$ inside $\mathbb{D}$ (Figure 3(b)). The right-hand side of equation (49) can be seen as (the Fourier transform of) the cross-correlation of these responses, integrated along the boundary $\partial\mathbb{D}$. The left-hand side is the retrieved homogeneous Green's matrix between $\mathbf{x}_A$ and $\mathbf{x}_B$. Hence, the receiver at $\mathbf{x}_A$ (on the right-hand side of this equation) is turned into a virtual source at $\mathbf{x}_A$ (on the left-hand side). When the sources at $\partial\mathbb{D}$ are uncorrelated noise sources, the right-hand side of equation (49) can be turned into a direct cross-correlation of the noise responses at $\mathbf{x}_A$ and $\mathbf{x}_B$, without needing an integral along the sources (similar as in references [64–68]; a further discussion of Green's matrix retrieval from ambient noise is beyond the scope of this paper).

For practical applications, a disadvantage of equations (48) and (49) is that the integration boundary $\partial\mathbb{D}$ consists of two boundaries, which together enclose $\mathbf{x}_A$ and $\mathbf{x}_B$. Hence, depending on the application, one needs either receivers (equation 48) or sources (equation 49) on both boundaries $\partial\mathbb{D}_-$ and $\partial\mathbb{D}_+$. In many practical situations, a medium is accessible from one side only, meaning that the integral can only be evaluated along a single boundary. For media with $\mathcal{PT}$-symmetry, the integral along the two-sided boundary $\partial\mathbb{D}$ can be turned into an integral along only one of the boundaries $\partial\mathbb{D}_-$ or $\partial\mathbb{D}_+$. We illustrate this for equation (49). Using that $n_3 = \pm 1$ at $\partial\mathbb{D}_\pm$, equation (49) can be rewritten as

$$\mathbf{G}_\mathrm{h}(\mathbf{x}_B, \mathbf{x}_A) = \int_{\partial\mathbb{D}_-} \mathbf{G}(\mathbf{x}_B, \mathbf{x})\mathbf{K}\bar{\mathbf{G}}^\dagger(\mathbf{x}_A, \mathbf{x})\mathbf{K}\mathrm{d}^2\mathbf{x}_\mathrm{H} - \int_{\partial\mathbb{D}_+} \mathbf{G}(\mathbf{x}_B, \mathbf{x})\mathbf{K}\bar{\mathbf{G}}^\dagger(\mathbf{x}_A, \mathbf{x})\mathbf{K}\mathrm{d}^2\mathbf{x}_\mathrm{H}. \tag{50}$$

For a $\mathcal{PT}$-symmetric medium we can use symmetry relations (36) and (42). Together with the aforementioned properties of $\mathbf{K}$ and $\mathbf{N}$ and $\mathbf{KN} = -\mathbf{J}$, we thus rewrite the integral along $\partial\mathbb{D}_+$ as

$$\begin{aligned}\int_{\partial\mathbb{D}_+} \mathbf{G}(\mathbf{x}_B, \mathbf{x})\mathbf{K}\bar{\mathbf{G}}^\dagger(\mathbf{x}_A, \mathbf{x})\mathbf{K}\mathrm{d}^2\mathbf{x}_\mathrm{H} &= -\int_{\partial\mathbb{D}_+} \mathbf{J}\bar{\mathbf{G}}(-\mathbf{x}_B, -\mathbf{x})\mathbf{K}\mathbf{G}^\dagger(-\mathbf{x}_A, -\mathbf{x})\mathbf{N}\mathrm{d}^2\mathbf{x}_\mathrm{H} \\ &= \int_{\partial\mathbb{D}_-} \mathbf{J}\bar{\mathbf{G}}(-\mathbf{x}_B, \mathbf{x})\mathbf{K}\mathbf{G}^\dagger(-\mathbf{x}_A, \mathbf{x})\mathbf{N}\mathrm{d}^2\mathbf{x}_\mathrm{H}. \end{aligned} \tag{51}$$

With this, equation (50) is turned into a single-sided integral, according to

$$\mathbf{G}_\mathrm{h}(\mathbf{x}_B, \mathbf{x}_A) = \int_{\partial\mathbb{D}_-} \Big(\mathbf{G}(\mathbf{x}_B, \mathbf{x})\mathbf{K}\bar{\mathbf{G}}^\dagger(\mathbf{x}_A, \mathbf{x})\mathbf{K} - \mathbf{J}\bar{\mathbf{G}}(-\mathbf{x}_B, \mathbf{x})\mathbf{K}\mathbf{G}^\dagger(-\mathbf{x}_A, \mathbf{x})\mathbf{N}\Big)\mathrm{d}^2\mathbf{x}_\mathrm{H}. \tag{52}$$

The evaluation of this integral requires observations at four positions in the $\mathcal{PT}$-symmetric medium and its adjoint (Figure 3(c)). For the special case that $\mathbf{x}_B = -\mathbf{x}_A$ and the medium is lossless, we obtain

$$\mathbf{G}_\mathrm{h}(-\mathbf{x}_A, \mathbf{x}_A) = \int_{\partial\mathbb{D}_-} \Big(\mathbf{G}(-\mathbf{x}_A, \mathbf{x})\mathbf{K}\mathbf{G}^\dagger(\mathbf{x}_A, \mathbf{x})\mathbf{K} - \mathbf{J}\mathbf{G}(\mathbf{x}_A, \mathbf{x})\mathbf{K}\mathbf{G}^\dagger(-\mathbf{x}_A, \mathbf{x})\mathbf{N}\Big)\mathrm{d}^2\mathbf{x}_\mathrm{H}. \tag{53}$$

This integral can be evaluated when observations at only two positions are available (Figure 3(d)).

Preprints (www.preprints.org) | NOT PEER-REVIEWED | Posted: 28 September 2022 doi:10.20944/preprints202209.0444.v1

6. Relations between reflection and transmission responses for $\mathcal{PT}$-symmetric media

In reference [32] we presented a systematic analysis of the relations between reflection and transmission responses of arbitrary inhomogeneous media. Here we extend this analysis for $\mathcal{PT}$-symmetric media.

Consider the configuration of Figure 1. We assume that in $\mathbb{D}$ (including $\partial\mathbb{D}$) we have a source-free 3D inhomogeneous medium. At and outside the boundary $\partial\mathbb{D}$ the medium is assumed homogeneous. Sources may be present outside $\partial\mathbb{D}$. When the medium in state A is the same as that in state B, we find for this situation from reciprocity theorems (16) and (17)

$$\int_{\partial\mathbb{D}} \mathbf{q}_A^t(\mathbf{x})\mathbf{N}\mathbf{q}_B(\mathbf{x})n_3\mathrm{d}^2\mathbf{x}_\mathrm{H} = 0 \tag{54}$$

and, assuming $\mathcal{PT}$-symmetry,

$$\int_{\partial\mathbb{D}} \mathbf{q}_A^\dagger(-\mathbf{x})\mathbf{N}\mathbf{q}_B(\mathbf{x})n_3\mathrm{d}^2\mathbf{x}_\mathrm{H} = 0, \tag{55}$$

respectively. On the other hand, when the medium in state A is the adjoint of that in state B, we find from reciprocity theorems (18) and (19)

$$\int_{\partial\mathbb{D}} \mathbf{q}_A^\dagger(\mathbf{x})\mathbf{K}\mathbf{q}_B(\mathbf{x})n_3\mathrm{d}^2\mathbf{x}_\mathrm{H} = 0 \tag{56}$$

and, assuming $\mathcal{PT}$-symmetry,

$$\int_{\partial\mathbb{D}} \mathbf{q}_A^t(-\mathbf{x})\mathbf{K}\mathbf{q}_B(\mathbf{x})n_3\mathrm{d}^2\mathbf{x}_\mathrm{H} = 0, \tag{57}$$

respectively. Using this in equations (28) $-$ (31), we find that the right-hand sides of these equations are also equal to zero. Dividing $\partial\mathbb{D}$ again into $\partial\mathbb{D}_-$ and $\partial\mathbb{D}_+$, with $n_3 = -1$ and $n_3 = +1$, respectively, we thus obtain

$$\int_{\partial\mathbb{D}_-} \Big(\{\mathbf{p}_A^+(\mathbf{x})\}^t\mathbf{p}_B^-(\mathbf{x}) - \{\mathbf{p}_A^-(\mathbf{x})\}^t\mathbf{p}_B^+(\mathbf{x})\Big)\mathrm{d}^2\mathbf{x}_\mathrm{H} = \int_{\partial\mathbb{D}_+} \Big(\{\mathbf{p}_A^+(\mathbf{x})\}^t\mathbf{p}_B^-(\mathbf{x}) - \{\mathbf{p}_A^-(\mathbf{x})\}^t\mathbf{p}_B^+(\mathbf{x})\Big)\mathrm{d}^2\mathbf{x}_\mathrm{H}, \tag{58}$$

$$\int_{\partial\mathbb{D}_-} \Big(\{\mathbf{p}_A^+(-\mathbf{x})\}^\dagger\mathbf{p}_B^-(\mathbf{x}) - \{\mathbf{p}_A^-(-\mathbf{x})\}^\dagger\mathbf{p}_B^+(\mathbf{x})\Big)\mathrm{d}^2\mathbf{x}_\mathrm{H} = \int_{\partial\mathbb{D}_+} \Big(\{\mathbf{p}_A^+(-\mathbf{x})\}^\dagger\mathbf{p}_B^-(\mathbf{x}) - \{\mathbf{p}_A^-(-\mathbf{x})\}^\dagger\mathbf{p}_B^+(\mathbf{x})\Big)\mathrm{d}^2\mathbf{x}_\mathrm{H}, \tag{59}$$

$$\int_{\partial\mathbb{D}_-} \Big(\{\mathbf{p}_A^+(\mathbf{x})\}^\dagger\mathbf{p}_B^+(\mathbf{x}) - \{\mathbf{p}_A^-(\mathbf{x})\}^\dagger\mathbf{p}_B^-(\mathbf{x})\Big)\mathrm{d}^2\mathbf{x}_\mathrm{H} = \int_{\partial\mathbb{D}_+} \Big(\{\mathbf{p}_A^+(\mathbf{x})\}^\dagger\mathbf{p}_B^+(\mathbf{x}) - \{\mathbf{p}_A^-(\mathbf{x})\}^\dagger\mathbf{p}_B^-(\mathbf{x})\Big)\mathrm{d}^2\mathbf{x}_\mathrm{H}, \tag{60}$$

$$\int_{\partial\mathbb{D}_-} \Big(\{\mathbf{p}_A^+(-\mathbf{x})\}^t\mathbf{p}_B^+(\mathbf{x}) - \{\mathbf{p}_A^-(-\mathbf{x})\}^t\mathbf{p}_B^-(\mathbf{x})\Big)\mathrm{d}^2\mathbf{x}_\mathrm{H} = \int_{\partial\mathbb{D}_+} \Big(\{\mathbf{p}_A^+(-\mathbf{x})\}^t\mathbf{p}_B^+(\mathbf{x}) - \{\mathbf{p}_A^-(-\mathbf{x})\}^t\mathbf{p}_B^-(\mathbf{x})\Big)\mathrm{d}^2\mathbf{x}_\mathrm{H}. \tag{61}$$

Equations (58) and (60) hold for arbitrary inhomogeneous media in $\mathbb{D}$, whereas $\mathcal{PT}$-symmetry is assumed for equations (59) and (61). Equations (58) and (59) hold when the medium in state A is the same as that in state B, whereas the underlying assumption for equations (60) and (61) is that the medium in state A is the adjoint of that in state B.

Next, we define the states to which these reciprocity theorems will be applied. For state $A1$ (Figure 4(a)) we choose a unit source for downgoing waves at $\mathbf{x}_A$, just above $\partial\mathbb{D}_-$. The downgoing field $\mathbf{p}_A^+$ at $\partial\mathbb{D}_-$, i.e., just below the source, is $\mathbf{I}\delta(\mathbf{x}_\mathrm{H} - \mathbf{x}_{\mathrm{H},A})$, where $\mathbf{x}_{\mathrm{H},A}$ denotes the horizontal coordinates of $\mathbf{x}_A$. The upgoing field $\mathbf{p}_A^-$ at $\partial\mathbb{D}_-$ is the reflection response $\mathbf{R}^\cup(\mathbf{x},\mathbf{x}_A)$ (the symbol $\mathbf{R}^\cup$ standing for "reflection from above") and the downgoing field $\mathbf{p}_A^+$ at $\partial\mathbb{D}_+$ is the transmission response $\mathbf{T}^\downarrow(\mathbf{x},\mathbf{x}_A)$. At $\partial\mathbb{D}_+$ there is no upgoing field. The fields in state $A1$ are summarized in the upper-left part of Table 2. For state $A2$ (Figure 4(b)) we choose a unit source for upgoing waves at $\mathbf{x}'_A$, just below $\partial\mathbb{D}_+$. The upgoing field $\mathbf{p}_A^-$ at $\partial\mathbb{D}_+$, i.e., just above the source, is $\mathbf{I}\delta(\mathbf{x}_\mathrm{H} - \mathbf{x}'_{\mathrm{H},A})$, where $\mathbf{x}'_{\mathrm{H},A}$ denotes the horizontal coordinates of $\mathbf{x}'_A$. The downgoing field $\mathbf{p}_A^+$ at $\partial\mathbb{D}_+$ is the reflection response $\mathbf{R}^\cap(\mathbf{x},\mathbf{x}'_A)$ (the symbol $\mathbf{R}^\cap$ standing for "reflection from below") and the upgoing field $\mathbf{p}_A^-$ at $\partial\mathbb{D}_-$ is the

Preprints (www.preprints.org) | NOT PEER-REVIEWED | Posted: 28 September 2022 doi:10.20944/preprints202209.0444.v1

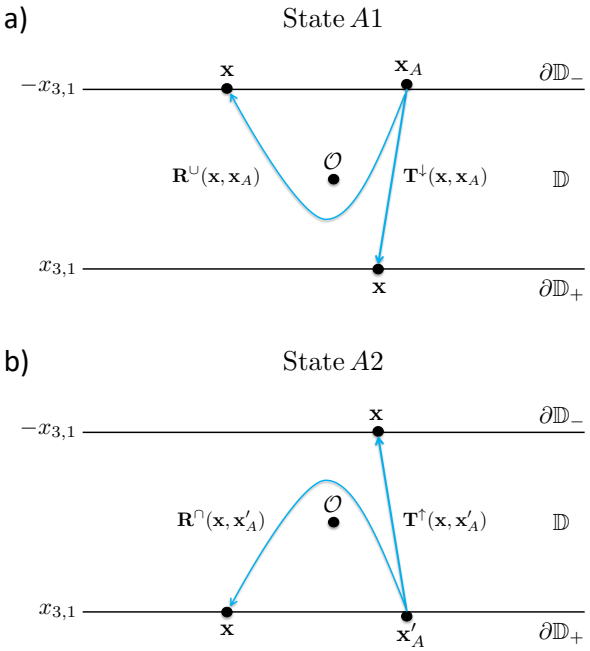

Figure 4. States for the derivation of relations between reflection and transmission responses from reciprocity theorems (58) − (61). (a) State $A1$: the source at $\mathbf{x}_A$ is situated just above $\partial\mathbb{D}_-$. The responses at $\partial\mathbb{D}_-$ and $\partial\mathbb{D}_+$ are the reflection response $\mathbf{R}^{\cup}(\mathbf{x},\mathbf{x}_A)$ and the transmission response $\mathbf{T}^{\downarrow}(\mathbf{x},\mathbf{x}_A)$. (b) State $A2$: the source at $\mathbf{x}'_A$ is situated just below $\partial\mathbb{D}_+$. The responses at $\partial\mathbb{D}_+$ and $\partial\mathbb{D}_-$ are the reflection response $\mathbf{R}^{\cap}(\mathbf{x},\mathbf{x}'_A)$ and the transmission response $\mathbf{T}^{\uparrow}(\mathbf{x},\mathbf{x}'_A)$.

transmission response $\mathbf{T}^{\uparrow}(\mathbf{x},\mathbf{x}'_A)$. At $\partial\mathbb{D}_-$ there is no downgoing field. The fields in state $A2$ are summarized in the lower-left part of Table 2. States $B1$ and $B2$ are defined in the same way, except that all subscripts A are replaced by subscripts B (see the upper-right and lower-right parts of Table 2).

In the following derivations, keep in mind that $\mathbf{x}_A$ and $\mathbf{x}_B$ are both just above $\partial\mathbb{D}_-$, whereas $\mathbf{x}'_A$ and $\mathbf{x}'_B$ are both just below $\partial\mathbb{D}_+$. Consequently, $-\mathbf{x}_A$ and $-\mathbf{x}_B$ are both just below $\partial\mathbb{D}_+$, whereas $-\mathbf{x}'_A$ and $-\mathbf{x}'_B$ are both just above $\partial\mathbb{D}_-$. Finally, when variable $\mathbf{x}$ is at $\partial\mathbb{D}_-$, then $-\mathbf{x}$ is at $\partial\mathbb{D}_+$ and vice versa.

We substitute combinations of A and B states into the reciprocity theorems (58) − (61). We start with substitutions in reciprocity theorem (58). Substituting states $A1$ and $B1$ yields

$$\mathbf{R}^{\cup}(\mathbf{x}_A,\mathbf{x}_B) = \{\mathbf{R}^{\cup}(\mathbf{x}_B,\mathbf{x}_A)\}^t. \tag{62}$$

Table 2. States for the derivation of relations between reflection and transmission responses from reciprocity theorems (58) − (61).

State $A1$	$\mathbf{p}_A^+(\mathbf{x})$	$\mathbf{p}_A^-(\mathbf{x})$	State $B1$	$\mathbf{p}_B^+(\mathbf{x})$	$\mathbf{p}_B^-(\mathbf{x})$
$\mathbf{x}$ at $\partial\mathbb{D}_-$	$\mathbf{I}\delta(\mathbf{x}_{\mathrm{H}}-\mathbf{x}_{\mathrm{H},A})$	$\mathbf{R}^{\cup}(\mathbf{x},\mathbf{x}_A)$	$\mathbf{x}$ at $\partial\mathbb{D}_-$	$\mathbf{I}\delta(\mathbf{x}_{\mathrm{H}}-\mathbf{x}_{\mathrm{H},B})$	$\mathbf{R}^{\cup}(\mathbf{x},\mathbf{x}_B)$
$\mathbf{x}$ at $\partial\mathbb{D}_+$	$\mathbf{T}^{\downarrow}(\mathbf{x},\mathbf{x}_A)$	$\mathbf{O}$	$\mathbf{x}$ at $\partial\mathbb{D}_+$	$\mathbf{T}^{\downarrow}(\mathbf{x},\mathbf{x}_B)$	$\mathbf{O}$

State $A2$	$\mathbf{p}_A^+(\mathbf{x})$	$\mathbf{p}_A^-(\mathbf{x})$	State $B2$	$\mathbf{p}_B^+(\mathbf{x})$	$\mathbf{p}_B^-(\mathbf{x})$
$\mathbf{x}$ at $\partial\mathbb{D}_-$	$\mathbf{O}$	$\mathbf{T}^{\uparrow}(\mathbf{x},\mathbf{x}'_A)$	$\mathbf{x}$ at $\partial\mathbb{D}_-$	$\mathbf{O}$	$\mathbf{T}^{\uparrow}(\mathbf{x},\mathbf{x}'_B)$
$\mathbf{x}$ at $\partial\mathbb{D}_+$	$\mathbf{R}^{\cap}(\mathbf{x},\mathbf{x}'_A)$	$\mathbf{I}\delta(\mathbf{x}_{\mathrm{H}}-\mathbf{x}'_{\mathrm{H},A})$	$\mathbf{x}$ at $\partial\mathbb{D}_+$	$\mathbf{R}^{\cap}(\mathbf{x},\mathbf{x}'_B)$	$\mathbf{I}\delta(\mathbf{x}_{\mathrm{H}}-\mathbf{x}'_{\mathrm{H},B})$

Preprints (www.preprints.org) | NOT PEER-REVIEWED | Posted: 28 September 2022 doi:10.20944/preprints202209.0444.v1

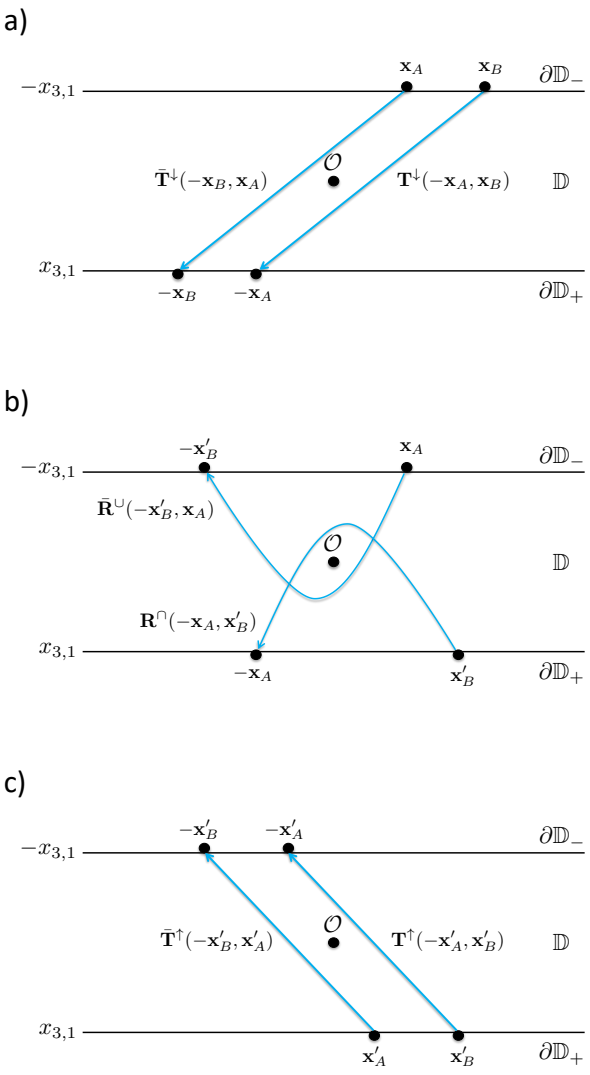

Figure 5. Additional source-receiver reciprocity of transmission and reflection responses for a medium with $\mathcal{PT}$-symmetry. (a) Equation (65). (b) Equation (66). (c) Equation (67).

Preprints (www.preprints.org) | NOT PEER-REVIEWED | Posted: 28 September 2022 doi:10.20944/preprints202209.0444.v1

States $A1$ and $B2$ substituted into equation (58) yields

$$\mathbf{T}^{\uparrow}(\mathbf{x}_A, \mathbf{x}'_B) = \{\mathbf{T}^{\downarrow}(\mathbf{x}'_B, \mathbf{x}_A)\}^t. \tag{63}$$

Substitution of states $A2$ and $B1$ yields a redundant relation which is not given here. Finally, substitution of states $A2$ and $B2$ into equation (58) yields

$$\mathbf{R}^{\cap}(\mathbf{x}'_A, \mathbf{x}'_B) = \{\mathbf{R}^{\cap}(\mathbf{x}'_B, \mathbf{x}'_A)\}^t. \tag{64}$$

Equations (62) $-$ (64) are the well-known source-receiver reciprocity relations for flux-normalised reflection and transmission responses of an arbitrary inhomogeneous medium.

Next, we use reciprocity theorem (61) to derive additional source-receiver reciprocity relations for these responses in a medium with $\mathcal{PT}$-symmetry. Substituting state $A1$ (in the adjoint medium) and state $B1$ (in the original medium) yields

$$\mathbf{T}^{\downarrow}(-\mathbf{x}_A, \mathbf{x}_B) = \{\bar{\mathbf{T}}^{\downarrow}(-\mathbf{x}_B, \mathbf{x}_A)\}^t. \tag{65}$$

State $A1$ (in the adjoint medium) and state $B2$ substituted into equation (61) yields

$$\mathbf{R}^{\cap}(-\mathbf{x}_A, \mathbf{x}'_B) = \{\bar{\mathbf{R}}^{\cup}(-\mathbf{x}'_B, \mathbf{x}_A)\}^t. \tag{66}$$

We skip the redundant relation which is obtained by substituting states $A2$ and state $B1$. Finally, substitution of state $A2$ (in the adjoint medium) and state $B2$ into equation (61) yields

$$\mathbf{T}^{\uparrow}(-\mathbf{x}'_A, \mathbf{x}'_B) = \{\bar{\mathbf{T}}^{\uparrow}(-\mathbf{x}'_B, \mathbf{x}'_A)\}^t. \tag{67}$$

Equations (65) $-$ (67) are illustrated in Figure 5.

Next, we derive two relations using reciprocity theorem (60). Substitution of state $A1$ (in the adjoint medium) and state $B1$ yields

$$\int_{\partial\mathbb{D}_+} \{\bar{\mathbf{T}}^{\downarrow}(\mathbf{x}, \mathbf{x}_A)\}^{\dagger} \mathbf{T}^{\downarrow}(\mathbf{x}, \mathbf{x}_B) \mathrm{d}^2\mathbf{x}_{\mathrm{H}} = \mathbf{I}\delta(\mathbf{x}_{\mathrm{H},A} - \mathbf{x}_{\mathrm{H},B}) - \int_{\partial\mathbb{D}_-} \{\bar{\mathbf{R}}^{\cup}(\mathbf{x}, \mathbf{x}_A)\}^{\dagger} \mathbf{R}^{\cup}(\mathbf{x}, \mathbf{x}_B) \mathrm{d}^2\mathbf{x}_{\mathrm{H}}. \tag{68}$$

This relation is a generalisation to an arbitrary inhomogeneous medium of the energy conservation relation $|T|^2 = 1 - |R|^2$ for a lossless layered medium. In its general form it can be used to derive properties of the transmission response from the reflection response measured at $\partial\mathbb{D}_-$. Substituting state $A1$ (in the adjoint medium) and state $B2$ into equation (60) yields

$$\int_{\partial\mathbb{D}_-} \{\bar{\mathbf{R}}^{\cup}(\mathbf{x}, \mathbf{x}_A)\}^{\dagger} \mathbf{T}^{\uparrow}(\mathbf{x}, \mathbf{x}'_B) \mathrm{d}^2\mathbf{x}_{\mathrm{H}} = -\int_{\partial\mathbb{D}_+} \{\bar{\mathbf{T}}^{\downarrow}(\mathbf{x}, \mathbf{x}_A)\}^{\dagger} \mathbf{R}^{\cap}(\mathbf{x}, \mathbf{x}'_B) \mathrm{d}^2\mathbf{x}_{\mathrm{H}}. \tag{69}$$

This expression relates reflection and transmission responses of an arbitrary inhomogeneous medium. Substitution of other combinations of the states in Table 2 into equation (60) yields relations similar to equations (68) and (69), which are not explicitly give here.

Finally, we derive two more relations for media with $\mathcal{PT}$-symmetry, using reciprocity theorem (59). Substitution of states $A1$ and $B1$ yields the following relation between reflection and transmission responses

$$\int_{\partial\mathbb{D}_-} \{\mathbf{T}^{\downarrow}(-\mathbf{x}, \mathbf{x}_A)\}^{\dagger} \mathbf{R}^{\cup}(\mathbf{x}, \mathbf{x}_B) \mathrm{d}^2\mathbf{x}_{\mathrm{H}} = -\int_{\partial\mathbb{D}_+} \{\mathbf{R}^{\cup}(-\mathbf{x}, \mathbf{x}_A)\}^{\dagger} \mathbf{T}^{\downarrow}(\mathbf{x}, \mathbf{x}_B) \mathrm{d}^2\mathbf{x}_{\mathrm{H}}, \tag{70}$$

whereas substitution of states $A1$ and $B2$ gives

$$\int_{\partial\mathbb{D}_-} \{\mathbf{T}^{\downarrow}(-\mathbf{x}, \mathbf{x}_A)\}^{\dagger} \mathbf{T}^{\uparrow}(\mathbf{x}, \mathbf{x}'_B) \mathrm{d}^2\mathbf{x}_{\mathrm{H}} = \mathbf{I}\delta(-\mathbf{x}_{\mathrm{H},A} - \mathbf{x}'_{\mathrm{H},B}) - \int_{\partial\mathbb{D}_+} \{\mathbf{R}^{\cup}(-\mathbf{x}, \mathbf{x}_A)\}^{\dagger} \mathbf{R}^{\cap}(\mathbf{x}, \mathbf{x}'_B) \mathrm{d}^2\mathbf{x}_{\mathrm{H}}. \tag{71}$$

Preprints (www.preprints.org) | NOT PEER-REVIEWED | Posted: 28 September 2022 doi:10.20944/preprints202209.0444.v1

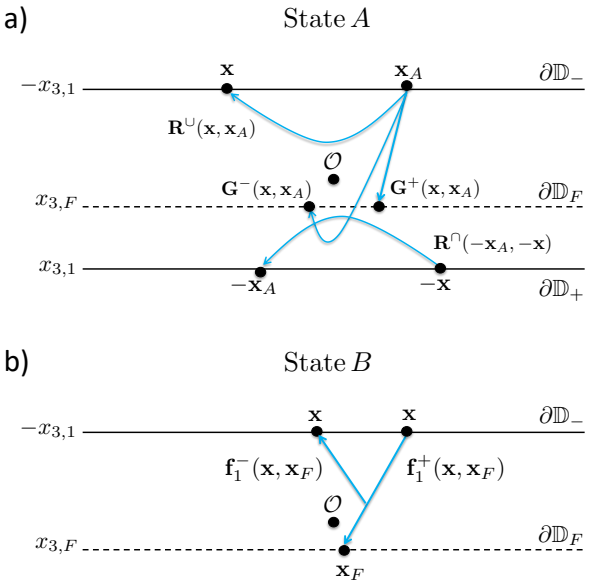

Figure 6. States for the derivation of Marchenko-type representations. (a) State A: the source at $\mathbf{x}_A$ is situated just above $\partial\mathbb{D}_-$. The response at $\partial\mathbb{D}_-$ is the reflection response $\mathbf{R}^{\cup}(\mathbf{x},\mathbf{x}_A)$ and the response at the focal depth level $\partial\mathbb{D}_F$ consists of the downgoing and upgoing Green's matrices $\mathbf{G}^+(\mathbf{x},\mathbf{x}_A)$ and $\mathbf{G}^-(\mathbf{x},\mathbf{x}_A)$, respectively. (b) State B: the focal point $\mathbf{x}_F$ is situated at $\partial\mathbb{D}_F$. At $\partial\mathbb{D}_-$ the focusing matrix consists of downgoing and upgoing parts $\mathbf{f}_1^+(\mathbf{x},\mathbf{x}_F)$ and $\mathbf{f}_1^-(\mathbf{x},\mathbf{x}_F)$, respectively. The medium below $\partial\mathbb{D}_F$ is reflection-free for this state.

The latter expression is a generalisation to an inhomogeneous $\mathcal{PT}$-symmetric medium of the unitarity relation $|T|^2 = 1 - R_L^* R_R$ for a layered $\mathcal{PT}$-symmetric medium [3,8]. Substitution of other combinations of states into equation (59) gives similar relations, which will not be discussed.

7. Marchenko method for $\mathcal{PT}$ media with double-sided access

Building on work by Marchenko [69], geophysicists recently developed a methodology to retrieve the wave field inside a 3D inhomogeneous medium from reflection measurements at its boundary [33,70–76]. Underlying this methodology are representations for Green's functions in terms of the reflection response and focusing functions [34,35]. Here we review these representations, modify them for $\mathcal{PT}$-symmetric media, discuss a modified Marchenko method and illustrate it with a simple numerical example.

We define a focal point $\mathbf{x}_F = (x_{1,F}, x_{2,F}, x_{3,F})$, with $x_{3,F}$ somewhere between $-x_{3,1}$ and $x_{3,1}$. This time we will apply the reciprocity theorems to a modified domain, enclosed by $\partial\mathbb{D}_-$ and $\partial\mathbb{D}_F$, with the latter boundary chosen at $x_{3,F}$ (hence, we replace $\partial\mathbb{D}_+$ by $\partial\mathbb{D}_F$ in the reciprocity theorems). For state A (Figure 6(a)) we choose again a unit source for downgoing waves at $\mathbf{x}_A$, just above $\partial\mathbb{D}_-$. The downgoing field $\mathbf{p}_A^+$ at $\partial\mathbb{D}_-$, i.e., just below the source, is $\mathbf{I}\delta(\mathbf{x}_{\mathrm{H}} - \mathbf{x}_{\mathrm{H},A})$ and the upgoing field $\mathbf{p}_A^-$ at $\partial\mathbb{D}_-$ is the reflection response $\mathbf{R}^{\cup}(\mathbf{x},\mathbf{x}_A)$. The response at $\partial\mathbb{D}_F$ consists of the downgoing and upgoing parts of the Green's matrix, i.e., $\mathbf{G}^+(\mathbf{x},\mathbf{x}_A)$ and $\mathbf{G}^-(\mathbf{x},\mathbf{x}_A)$, respectively. The fields in state A are summarized in the left part of Table 3. For state B (Figure 6(b)) we choose a focusing matrix $\mathbf{f}_1(\mathbf{x},\mathbf{x}_F)$ defined in a medium which is reflection-free below the focusing depth level $\partial\mathbb{D}_F$. At $\partial\mathbb{D}_-$ this focusing matrix consists of downgoing and upgoing parts $\mathbf{f}_1^+(\mathbf{x},\mathbf{x}_F)$ and $\mathbf{f}_1^-(\mathbf{x},\mathbf{x}_F)$, respectively. It is defined such that it focuses at $\partial\mathbb{D}_F$, hence $\mathbf{f}_1^+(\mathbf{x},\mathbf{x}_F) = \mathbf{I}\delta(\mathbf{x}_{\mathrm{H}} - \mathbf{x}_{\mathrm{H},F})$ for $\mathbf{x}$ at $\partial\mathbb{D}_F$, where $\mathbf{x}_{\mathrm{H},F}$ denotes the horizontal coordinates of $\mathbf{x}_F$. Since the medium below $\partial\mathbb{D}_F$ is reflection-free, we have $\mathbf{f}_1^-(\mathbf{x},\mathbf{x}_F) = \mathbf{O}$ for $\mathbf{x}$ at $\partial\mathbb{D}_F$. The fields in state B are summarized in the right part of Table 3.

Preprints (www.preprints.org) | NOT PEER-REVIEWED | Posted: 28 September 2022 doi:10.20944/preprints202209.0444.v1

Table 3. States for the derivation of Marchenko-type representations.

State A	$\mathbf{p}_A^+(\mathbf{x})$	$\mathbf{p}_A^-(\mathbf{x})$	State B	$\mathbf{p}_B^+(\mathbf{x})$	$\mathbf{p}_B^-(\mathbf{x})$
$\mathbf{x}$ at $\partial\mathbb{D}_-$	$\mathbf{I}\delta(\mathbf{x}_\mathrm{H}-\mathbf{x}_{\mathrm{H},A})$	$\mathbf{R}^\cup(\mathbf{x},\mathbf{x}_A)$	$\mathbf{x}$ at $\partial\mathbb{D}_-$	$\mathbf{f}_1^+(\mathbf{x},\mathbf{x}_F)$	$\mathbf{f}_1^-(\mathbf{x},\mathbf{x}_F)$
$\mathbf{x}$ at $\partial\mathbb{D}_F$	$\mathbf{G}^+(\mathbf{x},\mathbf{x}_A)$	$\mathbf{G}^-(\mathbf{x},\mathbf{x}_A)$	$\mathbf{x}$ at $\partial\mathbb{D}_F$	$\mathbf{I}\delta(\mathbf{x}_\mathrm{H}-\mathbf{x}_{\mathrm{H},F})$	$\mathbf{O}$

Substituting states A and B into equation (58) (with $\partial\mathbb{D}_+$ replaced by $\partial\mathbb{D}_F$) yields

$$\{\mathbf{G}^-(\mathbf{x}_F,\mathbf{x}_A)\}^t+\mathbf{f}_1^-(\mathbf{x}_A,\mathbf{x}_F)=\int_{\partial\mathbb{D}_-}\{\mathbf{R}^\cup(\mathbf{x},\mathbf{x}_A)\}^t\mathbf{f}_1^+(\mathbf{x},\mathbf{x}_F)\mathrm{d}^2\mathbf{x}_\mathrm{H}. \tag{72}$$

Substitution of state A (in the adjoint medium) and state B into equation (60) yields

$$-\{\bar{\mathbf{G}}^+(\mathbf{x}_F,\mathbf{x}_A)\}^\dagger+\mathbf{f}_1^+(\mathbf{x}_A,\mathbf{x}_F)=\int_{\partial\mathbb{D}_-}\{\bar{\mathbf{R}}^\cup(\mathbf{x},\mathbf{x}_A)\}^\dagger\mathbf{f}_1^-(\mathbf{x},\mathbf{x}_F)\mathrm{d}^2\mathbf{x}_\mathrm{H}. \tag{73}$$

In most papers on the Marchenko method, the medium is assumed lossless. In that case the adjoint medium is the same as the actual medium, meaning that the bars in equation (73) can be omitted, hence, one-and-the-same reflection response $\mathbf{R}^\cup(\mathbf{x},\mathbf{x}_A)$ appears in equations (72) and (73). Slob [77] extended the Marchenko method for dissipative media, using (scalar versions of) equations (72) and (73), including the bars. His method requires the reflection response $\mathbf{R}^\cup(\mathbf{x},\mathbf{x}_A)$ in the actual (dissipative) medium and $\bar{\mathbf{R}}^\cup(\mathbf{x},\mathbf{x}_A)$ in the adjoint (effectual) medium. The former is obtained from measurements, the latter has to be obtained in a different way. Slob [77] proposes to measure the reflection response $\mathbf{R}^\cap$ from below (next to the reflection response $\mathbf{R}^\cup$ from above), and the transmission responses $\mathbf{T}^\downarrow$ and $\mathbf{T}^\uparrow$. Having these responses, $\bar{\mathbf{R}}^\cup$ can be obtained by solving equations (68) and (69).

For $\mathcal{PT}$-symmetric media, $\bar{\mathbf{R}}^\cup$ at $\partial\mathbb{D}_-$ can be obtained directly from $\mathbf{R}^\cap$ at $\partial\mathbb{D}_+$ (Figure 6(a)), using equation (66). Substituting this into equation (73) (and equation (62) into equation (72)) yields

$$\{\mathbf{G}^-(\mathbf{x}_F,\mathbf{x}_A)\}^t+\mathbf{f}_1^-(\mathbf{x}_A,\mathbf{x}_F)=\int_{\partial\mathbb{D}_-}\mathbf{R}^\cup(\mathbf{x}_A,\mathbf{x})\mathbf{f}_1^+(\mathbf{x},\mathbf{x}_F)\mathrm{d}^2\mathbf{x}_\mathrm{H} \tag{74}$$

and

$$-\{\bar{\mathbf{G}}^+(\mathbf{x}_F,\mathbf{x}_A)\}^\dagger+\mathbf{f}_1^+(\mathbf{x}_A,\mathbf{x}_F)=\int_{\partial\mathbb{D}_-}\{\mathbf{R}^\cap(-\mathbf{x}_A,-\mathbf{x})\}^*\mathbf{f}_1^-(\mathbf{x},\mathbf{x}_F)\mathrm{d}^2\mathbf{x}_\mathrm{H}. \tag{75}$$

Equations (74) and (75) form the basis for the Marchenko method in a $\mathcal{PT}$-symmetric medium. The approach is similar to that for lossy media [77], except that here we have replaced $\bar{\mathbf{R}}^\cup$ by $\mathbf{R}^\cap$. Starting with an estimate of the direct arrival of the focusing matrix, $\mathbf{f}_{1,\mathrm{d}}^+$, the Marchenko method leads to the retrieval of $\mathbf{G}^-$ and $\bar{\mathbf{G}}^+$, the latter in the adjoint medium. To retrieve $\mathbf{G}^+$ in the actual medium, we need a second set of equations. To this end, we replace all quantities in equations (74) and (75) by quantities in the adjoint medium (which implies that $\bar{\mathbf{G}}^+$ is replaced by $\mathbf{G}^+$). Using equations (62) and (66) this yields

$$\{\bar{\mathbf{G}}^-(\mathbf{x}_F,\mathbf{x}_A)\}^t+\bar{\mathbf{f}}_1^-(\mathbf{x}_A,\mathbf{x}_F)=\int_{\partial\mathbb{D}_-}\mathbf{R}^\cap(-\mathbf{x}_A,-\mathbf{x})\bar{\mathbf{f}}_1^+(\mathbf{x},\mathbf{x}_F)\mathrm{d}^2\mathbf{x}_\mathrm{H} \tag{76}$$

and

$$-\{\mathbf{G}^+(\mathbf{x}_F,\mathbf{x}_A)\}^\dagger+\bar{\mathbf{f}}_1^+(\mathbf{x}_A,\mathbf{x}_F)=\int_{\partial\mathbb{D}_-}\{\mathbf{R}^\cup(\mathbf{x}_A,\mathbf{x})\}^*\bar{\mathbf{f}}_1^-(\mathbf{x},\mathbf{x}_F)\mathrm{d}^2\mathbf{x}_\mathrm{H}. \tag{77}$$

Starting with an estimate of $\bar{\mathbf{f}}_{1,\mathrm{d}}^+$, the Marchenko method leads to the retrieval of $\bar{\mathbf{G}}^-$ and $\mathbf{G}^+$.

Preprints (www.preprints.org) | NOT PEER-REVIEWED | Posted: 28 September 2022 doi:10.20944/preprints202209.0444.v1

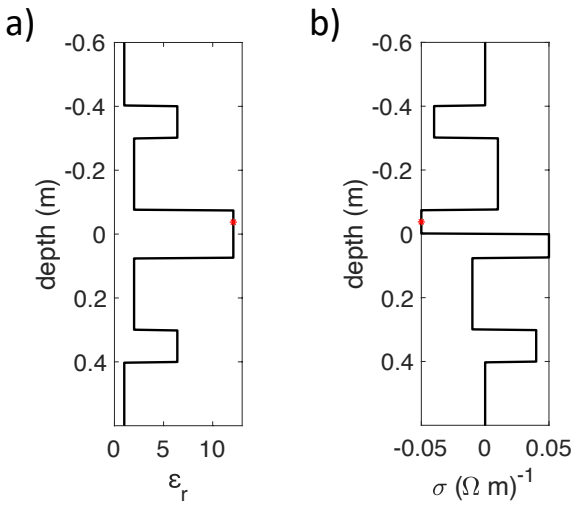

Figure 7. Parameters of a horizontally layered $\mathcal{PT}$-symmetric medium. The red stars indicate the focal depth $x_{3,F}$.

We illustrate this with a numerical example for electromagnetic waves in a horizontally layered $\mathcal{PT}$-symmetric medium. Figure 7(a) shows the relative permittivity $\varepsilon_r(x_3) = \varepsilon(x_3)/\varepsilon_0$ (with ε_0 the permittivity of vacuum) and Figure 7(b) the conductivity $\sigma(x_3)$. Both functions are chosen real-valued and frequency-independent. Note that $\varepsilon_r(x_3)$ is symmetric and $\sigma(x_3)$ is asymmetric. Hence, for $\mathcal{E}$ defined in equation (6) we have $\mathcal{E}(-x_3,\omega) = \bar{\mathcal{E}}(x_3,\omega) = \mathcal{E}^*(x_3,\omega)$. The relative permeability $\mu_r(x_3)$ is set to $\mu_r = 1$.

We define the spatial Fourier transform of a space- and frequency-dependent function $u(\mathbf{x},\omega)$ along the horizontal coordinate vector $\mathbf{x}_H$ as

$$\tilde{u}(\mathbf{s},x_3,\omega) = \int_{\mathbb{R}^2} \exp\{-i\omega\mathbf{s}\cdot\mathbf{x}_H\}u(\mathbf{x}_H,x_3,\omega)\mathrm{d}^2\mathbf{x}_H, \tag{78}$$

with $\mathbf{s} = (s_1, s_2)$, where s_1 and s_2 are horizontal slownesses and $\mathbb{R}$ is the set of real numbers. Moreover, we define the inverse Fourier transform from frequency ω to intercept time τ as [78]

$$u(\mathbf{s},x_3,\tau) = \frac{1}{\pi}\Re\int_0^\infty \tilde{u}(\mathbf{s},x_3,\omega)\exp\{-i\omega\tau\}\mathrm{d}\omega. \tag{79}$$

Applying these transforms to equations (74) – (77) for $\mathbf{x}_F = (0,0,x_{3,F})$ and $\mathbf{x}_A = (\mathbf{x}_{H,A}, -x_{3,1})$ with variable $\mathbf{x}_{H,A}$, yields

$$\{\mathbf{G}^-(-\mathbf{s},x_{3,F},-x_{3,1},\tau)\}^t + \mathbf{f}_1^-(\mathbf{s},-x_{3,1},x_{3,F},\tau) = \int_0^\infty \mathbf{R}^\cup(\mathbf{s},-x_{3,1},\tau')\mathbf{f}_1^+(\mathbf{s},-x_{3,1},x_{3,F},\tau-\tau')\mathrm{d}\tau', \tag{80}$$

$$-\{\bar{\mathbf{G}}^+(\mathbf{s},x_{3,F},-x_{3,1},-\tau)\}^t + \mathbf{f}_1^+(\mathbf{s},-x_{3,1},x_{3,F},\tau) = \int_0^\infty \mathbf{R}^\cap(\mathbf{s},x_{3,1},\tau')\mathbf{f}_1^-(\mathbf{s},-x_{3,1},x_{3,F},\tau+\tau')\mathrm{d}\tau', \tag{81}$$

$$\{\bar{\mathbf{G}}^-(-\mathbf{s},x_{3,F},-x_{3,1},\tau)\}^t + \bar{\mathbf{f}}_1^-(\mathbf{s},-x_{3,1},x_{3,F},\tau) = \int_0^\infty \mathbf{R}^\cap(-\mathbf{s},x_{3,1},\tau')\bar{\mathbf{f}}_1^+(\mathbf{s},-x_{3,1},x_{3,F},\tau-\tau')\mathrm{d}\tau', \tag{82}$$

$$-\{\mathbf{G}^+(\mathbf{s},x_{3,F},-x_{3,1},-\tau)\}^t + \bar{\mathbf{f}}_1^+(\mathbf{s},-x_{3,1},x_{3,F},\tau) = \int_0^\infty \mathbf{R}^\cup(-\mathbf{s},-x_{3,1},\tau')\bar{\mathbf{f}}_1^-(\mathbf{s},-x_{3,1},x_{3,F},\tau+\tau')\mathrm{d}\tau'. \tag{83}$$

Taking the horizontal slowness s_2 equal to 0, the transverse electric (TE) mode decouples from the transverse magnetic (TM) mode. Consequently, the matrices in equations (80) – (83) diagonalize. We continue with the upper-left elements of these matrices, which correspond to the up/down decomposed TE-mode. Figure 8(a) shows the scalar reflection response from above, $R^\cup(s_1,-x_{3,1},\tau)$, for $-x_{3,1} = -0.6$ m, as a function of intercept time

Preprints (www.preprints.org) | NOT PEER-REVIEWED | Posted: 28 September 2022 doi:10.20944/preprints202209.0444.v1

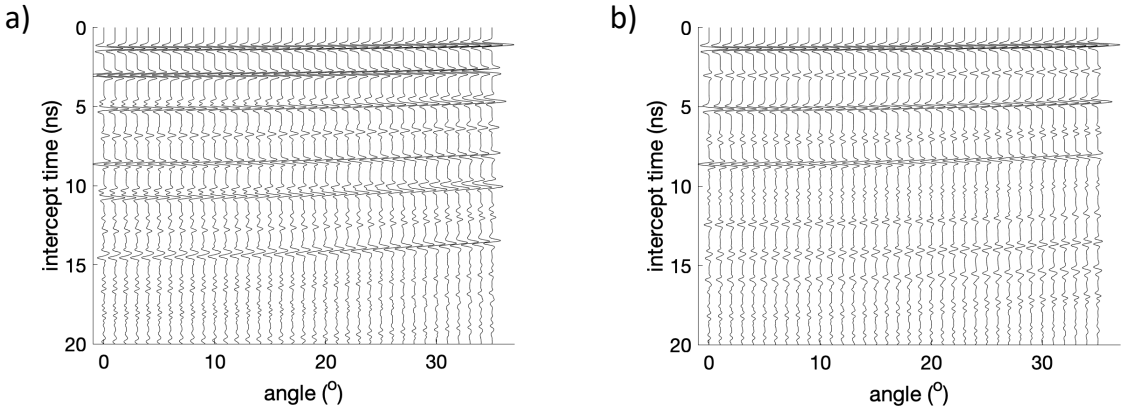

Figure 8. (a) Reflection response from above, $R^{\cup}(s_1, -x_{3,1}, \tau)$, for $-x_{3,1} = -0.6$ m. (b) Reflection response from below, $R^{\cap}(s_1, x_{3,1}, \tau)$, for $x_{3,1} = 0.6$ m.

τ and incidence angle θ. The latter is related to the horizontal slowness s_1 via $\frac{\sin\theta}{c} = s_1$, with c the propagation velocity at $-x_{3,1} = -0.6$ m (which is equal to the velocity of light in vacuum, since $\varepsilon_r = \mu_r = 1$ at $-x_{3,1} = -0.6$ m). Similarly, Figure 8(b) shows the scalar reflection response from below, $R^{\cap}(s_1, x_{3,1}, \tau)$, for $x_{3,1} = 0.6$ m. Both responses have been convolved with a symmetric source function with a central frequency of 2 GHz. Our aim is to use the Marchenko method to find the downgoing and upgoing parts of the Green's function, $G^{+}(s_1, x_{3,F}, -x_{3,1}, \tau)$ and $G^{-}(s_1, x_{3,F}, -x_{3,1}, \tau)$, between $-x_{3,1} = -0.6$ m and an arbitrary focal depth $x_{3,F}$ inside the medium, from the reflection responses $R^{\cup}$ and $R^{\cap}$. We discuss the main steps; for details on the Marchenko method, see the references at the beginning of this section. We choose the focal depth as $x_{3,F} = -3.75$ cm (indicated by the red stars in Figure 7). We apply a time window to suppress the Green's functions from equations (80) $-$ (83), which leaves equations for the focusing functions f_1^{+}, f_1^{-}, $\bar{f}_1^{+}$ and $\bar{f}_1^{-}$. We model the direct arrival $f_{1,\mathrm{d}}^{+}$ in the medium of Figure 7. Using this direct arrival as an initial estimate of f_1^{+}, the windowed versions of equations (80) and (81) are iteratively solved for f_1^{+} and f_1^{-}. Once these are found, the original versions of equations (80) and (81) (i.e., without the time window) yield estimates of G^{-} and $\bar{G}^{+}$. Next, we model the direct arrival $\bar{f}_{1,\mathrm{d}}^{+}$ in the adjoint of the medium of Figure 7 and use windowed versions of equations (82) and (83) to solve for $\bar{f}_1^{+}$ and $\bar{f}_1^{-}$ and, subsequently, retrieve estimates of $\bar{G}^{-}$ and G^{+}. The results G^{+} and G^{-} are shown by the red-dashed lines in Figures 9(a) and (b), respectively. The first arrival in G^{+} comes from $\bar{f}_{1,\mathrm{d}}^{+}$; all other (multiply reflected) arrivals have been retrieved from $R^{\cup}$ and $R^{\cap}$. The results are overlain on the directly modelled versions of G^{+} and G^{-} (black solid lines). Note that the match is excellent.

8. Discussion and conclusions

Starting with a unified matrix-vector wave equation for acoustic, quantum-mechanical, electromagnetic, elastodynamic, poroelastodynamic, piezoelectric and seismoelectric waves, we established symmetry properties of the operator matrix appearing in this equation for the situation of 3D arbitrary inhomogeneous media and for 3D inhomogeneous media with $\mathcal{PT}$-symmetry. For the latter situation we obtained an auxiliary matrix-vector wave equation. Exploiting the symmetry properties, we derived four unified reciprocity theorems, two for arbitrary inhomogeneous media and two for inhomogeneous media with $\mathcal{PT}$-symmetry. We used these reciprocity theorems to derive general wave field representations and relations between reflection and transmission responses, for 3D arbitrary inhomogeneous media and for 3D inhomogeneous media with $\mathcal{PT}$-symmetry. The latter generalise established relations, such as unitarity relations, to 3D inhomogeneous media. Finally, we modified the Marchenko method for retrieving Green's matrices from 3D inhomogeneous lossless media to 3D inhomogeneous media with $\mathcal{PT}$-symmetry.

Preprints (www.preprints.org) | NOT PEER-REVIEWED | Posted: 28 September 2022 doi:10.20944/preprints202209.0444.v1

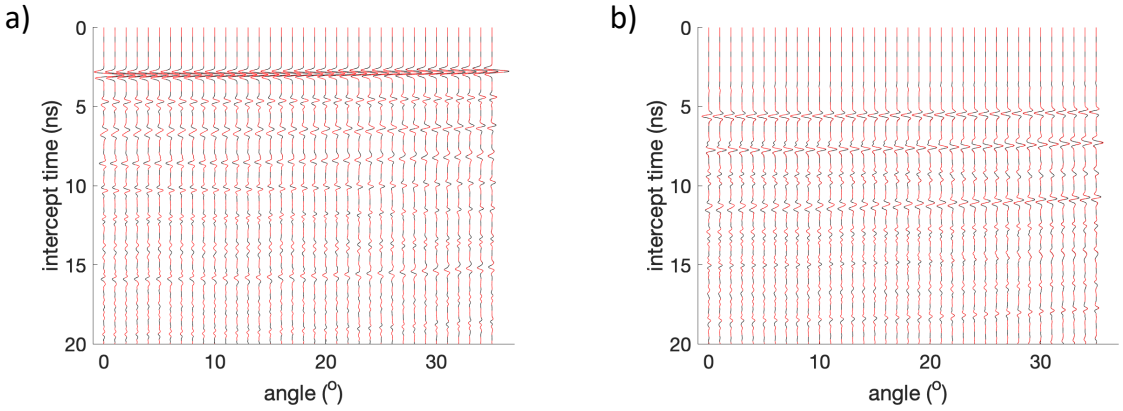

Figure 9. (a) Green's function $G^{+}(s_1, x_{3,F}, -x_{3,1}, \tau)$. (b) Green's function $G^{-}(s_1, x_{3,F}, -x_{3,1}, \tau)$. The red dashed lines are the Green's functions retrieved with the Marchenko method from $R^{\cup}$ and $R^{\cap}$; the black solid lines are the directly modelled Green's functions.

Given the current broad interest in applications of wave propagation and scattering in photonic structures, phononic crystals and acoustic metamaterials with $\mathcal{PT}$-symmetry, we hope that our unified formulation for different wave types and our generalisation for 3D inhomogeneous media with $\mathcal{PT}$-symmetry, will contribute to further developments in this interesting field of research.

Author Contributions: Conceptualization and methodology, K.W. and E.S.; software and validation, E.S.; writing—original draft preparation, review and editing, K.W.; funding acquisition, K.W. All authors have read and agreed to the published version of the manuscript.

Funding: This research is funded by the European Research Council (ERC) under the European Union's Horizon 2020 research and innovation programme (grant agreement No: 742703).

Data Availability Statement: Not applicable.

Acknowledgments: We thank Dirk-Jan van Manen (ETH Zürich) for bringing his research ideas to construct virtual $\mathcal{PT}$-symmetric media to our attention and for interesting discussions.

Conflicts of Interest: The authors declare no conflict of interest.

Appendix A. The operator matrix and its properties

Appendix A.1. The wave vector and operator matrix for different wave phenomena

For acoustic waves in an inhomogeneous fluid, p and v_3 in Table 1 are the acoustic pressure and the vertical component of the particle velocity, respectively. The 2×2 operator matrix $\boldsymbol{\mathcal{A}}(\mathbf{x})$ is defined as [42,79–82]

$$\boldsymbol{\mathcal{A}}(\mathbf{x}) = \begin{pmatrix} 0 & i\omega\rho \\ i\omega\kappa - \frac{1}{i\omega}\partial_\alpha \frac{1}{\rho}\partial_\alpha & 0 \end{pmatrix}, \tag{A1}$$

where $\kappa(\mathbf{x})$ is the compressibility and $\rho(\mathbf{x})$ the mass density.

For quantum-mechanical waves in an inhomogeneous potential, ψ and m in Table 1 are the wave function and the mass of a particle, respectively, and $\hbar = h/2\pi$, with h Planck's constant. The 2×2 matrix is [41,83,84]

$$\boldsymbol{\mathcal{A}}(\mathbf{x}) = \begin{pmatrix} 0 & \frac{mi}{2\hbar} \\ 4i\left(\omega - \frac{V}{\hbar}\right) - \frac{2\hbar}{mi}\partial_\alpha\partial_\alpha & 0 \end{pmatrix}, \tag{A2}$$

where $V(\mathbf{x})$ is the potential.

Preprints (www.preprints.org) | NOT PEER-REVIEWED | Posted: 28 September 2022 doi:10.20944/preprints202209.0444.v1

For electromagnetic waves in an inhomogeneous, isotropic medium, E_α and H_α ($\alpha = 1,2$) in Table 1 are the horizontal components of the electric and magnetic field strength, respectively. The 2×2 sub-matrices of operator matrix $\boldsymbol{\mathcal{A}}(\mathbf{x})$ are given by equations (4) and (5).

For elastodynamic waves in an inhomogeneous, isotropic solid, v_k and τ_{k3} ($k = 1,2,3$) in Table 1 are the particle velocity and traction components, respectively. The 3×3 sub-matrices are [39,42,52]

$$\boldsymbol{\mathcal{A}}_{11}(\mathbf{x}) = \begin{pmatrix} 0 & 0 & -\partial_1 \\ 0 & 0 & -\partial_2 \\ -\frac{\lambda}{\lambda+2\mu}\partial_1 & -\frac{\lambda}{\lambda+2\mu}\partial_2 & 0 \end{pmatrix}, \tag{A3}$$

$$\boldsymbol{\mathcal{A}}_{12}(\mathbf{x}) = \begin{pmatrix} \frac{i\omega}{\mu} & 0 & 0 \\ 0 & \frac{i\omega}{\mu} & 0 \\ 0 & 0 & \frac{i\omega}{\lambda+2\mu} \end{pmatrix}, \tag{A4}$$

$$\boldsymbol{\mathcal{A}}_{21}(\mathbf{x}) = \begin{pmatrix} i\omega\rho - \frac{1}{i\omega}\left(\partial_1\nu_1\partial_1 + \partial_2\mu\partial_2\right) & -\frac{1}{i\omega}\left(\partial_2\mu\partial_1 + \partial_1\nu_2\partial_2\right) & 0 \\ -\frac{1}{i\omega}\left(\partial_2\nu_2\partial_1 + \partial_1\mu\partial_2\right) & i\omega\rho - \frac{1}{i\omega}\left(\partial_1\mu\partial_1 + \partial_2\nu_1\partial_2\right) & 0 \\ 0 & 0 & i\omega\rho \end{pmatrix}, \tag{A5}$$

$$\boldsymbol{\mathcal{A}}_{22}(\mathbf{x}) = -\boldsymbol{\mathcal{A}}_{11}^t(\mathbf{x}), \tag{A6}$$

with

$$\nu_1 = 4\mu\left(\frac{\lambda+\mu}{\lambda+2\mu}\right), \quad \nu_2 = 2\mu\left(\frac{\lambda}{\lambda+2\mu}\right), \tag{A7}$$

where $\lambda(\mathbf{x})$ and $\mu(\mathbf{x})$ are the Lamé parameters and $\rho(\mathbf{x})$ the mass density.

The wave field quantities for the other wave phenomena in Table 1 are the same quantities as above, with superscripts b, f and s denoting that they are averaged in the bulk, fluid or solid, respectively; ϕ denotes porosity. For the sub-matrices for these phenomena we refer to the Appendices in reference [41].

Appendix A.2. Fourier transform of the operator matrix at the boundary

We assume that at the boundary $\partial\mathbb{D}$ the medium is laterally invariant. Applying the transform of equation (78) to the operator matrix of equation (A1) at the boundary $\partial\mathbb{D}$ yields

$$\tilde{\mathbf{A}}(\mathbf{s}, x_3) = \begin{pmatrix} 0 & i\omega\rho \\ i\omega\left(\kappa - \frac{1}{\rho}s_\alpha s_\alpha\right) & \end{pmatrix}, \tag{A8}$$

with $\kappa(x_3)$ and $\rho(x_3)$ for $x_3 = -x_{3,1}$ and $x_3 = x_{3,1}$ being the laterally invariant compressibility and mass density at the boundaries $\partial\mathbb{D}_-$ and $\partial\mathbb{D}_+$. Note that ∂_α has been replaced by $i\omega s_\alpha$. The operators for other wave phenomena are transformed in a similar way. The symmetry properties of equations (7), (8) and (9) transform to

$$\tilde{\mathbf{A}}^t(-\mathbf{s}, x_3)\mathbf{N} = -\mathbf{N}\tilde{\mathbf{A}}(\mathbf{s}, x_3), \tag{A9}$$

$$\tilde{\mathbf{A}}^\dagger(\mathbf{s}, x_3)\mathbf{K} = -\mathbf{K}\tilde{\mathbf{A}}(\mathbf{s}, x_3), \tag{A10}$$

$$\tilde{\mathbf{A}}^*(-\mathbf{s}, x_3)\mathbf{J} = \mathbf{J}\tilde{\tilde{\mathbf{A}}}(\mathbf{s}, x_3), \tag{A11}$$

for $x_3 = \pm x_{3,1}$. In equations (A10) and (A11), $\tilde{\tilde{\mathbf{A}}}(\mathbf{s}, x_3)$ is defined in the adjoint medium. For a $\mathcal{PT}$-symmetric medium, the symmetry property of equation (12) transforms to

$$\tilde{\mathbf{A}}(\mathbf{s}, -x_3) = -\tilde{\mathbf{A}}^*(\mathbf{s}, x_3), \tag{A12}$$

for $x_3 = \pm x_{3,1}$.

Preprints (www.preprints.org) | NOT PEER-REVIEWED | Posted: 28 September 2022 doi:10.20944/preprints202209.0444.v1

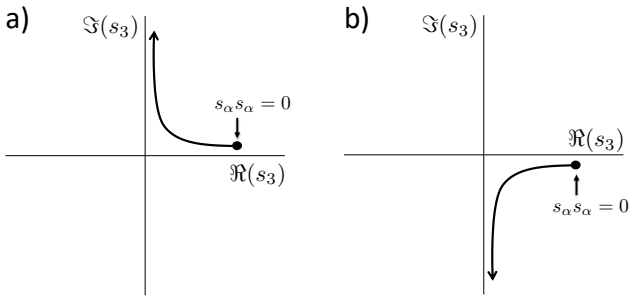

Figure A1. Slowness $s_3(\mathbf{s}, x_3)$ (for $x_3 = \pm x_{3,1}$) in the complex plane for a dissipative (a) and an effectual (b) medium.

Appendix A.3. Decomposition of the transformed operator matrix at the boundary

We define the eigenvalue decomposition of the transformed operator matrix at the boundary as

$$\tilde{\mathbf{A}}(\mathbf{s}, x_3) \quad = \quad \tilde{\mathbf{L}}(\mathbf{s}, x_3)\tilde{\mathbf{\Lambda}}(\mathbf{s}, x_3)\tilde{\mathbf{L}}^{-1}(\mathbf{s}, x_3), \tag{A13}$$

in which the matrices $\tilde{\mathbf{L}}(\mathbf{s}, x_3)$ and $\tilde{\mathbf{\Lambda}}(\mathbf{s}, x_3)$ are partitioned as follows

$$\tilde{\mathbf{L}}(\mathbf{s}, x_3) = \begin{pmatrix} \tilde{\mathbf{L}}_1^+ & \tilde{\mathbf{L}}_1^- \\ \tilde{\mathbf{L}}_2^+ & \tilde{\mathbf{L}}_2^- \end{pmatrix}, \quad \tilde{\mathbf{\Lambda}}(\mathbf{s}, x_3) = \begin{pmatrix} \tilde{\mathbf{\Lambda}}^+ & \mathbf{O} \\ \mathbf{O} & \tilde{\mathbf{\Lambda}}^- \end{pmatrix}, \tag{A14}$$

for $x_3 = \pm x_{3,1}$.

For acoustic waves we have

$$\tilde{\mathbf{L}}(\mathbf{s}, x_3) = \frac{1}{\sqrt{2}} \begin{pmatrix} \sqrt{\rho/s_3} & \sqrt{\rho/s_3} \\ \sqrt{s_3/\rho} & -\sqrt{s_3/\rho} \end{pmatrix}, \quad \tilde{\mathbf{\Lambda}}(\mathbf{s}, x_3) = \begin{pmatrix} i\omega s_3 & 0 \\ 0 & -i\omega s_3 \end{pmatrix}, \tag{A15}$$

where $s_3(\mathbf{s}, x_3)$ is the vertical slowness, defined as

$$s_3(\mathbf{s}, x_3) = \sqrt{\frac{1}{c^2(x_3)} - s_\alpha s_\alpha}, \quad c(x_3) = 1/\sqrt{\rho(x_3)\kappa(x_3)}, \tag{A16}$$

for $x_3 = \pm x_{3,1}$. When the medium is dissipative (with, for positive ω, $\Im(\kappa) > 0$ and $\Im(\rho) > 0$), we have $\Im(s_3) > 0$, see Figure A1(a). On the other hand, when the medium is effectual (with, for positive ω, $\Im(\kappa) < 0$ and $\Im(\rho) < 0$), we have $\Im(s_3) < 0$, see Figure A1(b). Since the parameters of the adjoint medium are defined as $\bar{\kappa} = \kappa^*$ and $\bar{\rho} = \rho^*$, the slowness $\bar{s}_3$ of the adjoint medium is given by $\bar{s}_3(\mathbf{s}, x_3) = s_3^*(\mathbf{s}, x_3)$ for $x_3 = \pm x_{3,1}$. For a $\mathcal{PT}$-symmetric medium we have in addition $\kappa(-x_3) = \kappa^*(x_3)$, $\rho(-x_3) = \rho^*(x_3)$ and hence $s_3(\mathbf{s}, -x_3) = s_3^*(\mathbf{s}, x_3)$ for $x_3 = \pm x_{3,1}$.

For quantum mechanical waves we have

$$\tilde{\mathbf{L}}(\mathbf{s}, x_3) = \frac{1}{\sqrt{2}} \begin{pmatrix} \sqrt{\frac{m}{2\hbar\omega s_3}} & \sqrt{\frac{m}{2\hbar\omega s_3}} \\ \sqrt{\frac{2\hbar\omega s_3}{m}} & -\sqrt{\frac{2\hbar\omega s_3}{m}} \end{pmatrix}, \tag{A17}$$

and $\tilde{\mathbf{\Lambda}}(\mathbf{s}, x_3)$ and $s_3(\mathbf{s}, x_3)$ defined as in equations (A15) and (A16), but with $c(x_3)$ defined as

$$c(x_3) = \sqrt{\frac{\hbar\omega}{2m(1 - \frac{V(x_3)}{\hbar\omega})}}, \tag{A18}$$

for $x_3 = \pm x_{3,1}$.

Preprints (www.preprints.org) | NOT PEER-REVIEWED | Posted: 28 September 2022 doi:10.20944/preprints202209.0444.v1

For electromagnetic waves, the sub-matrices are given by [42]

$$\tilde{\mathbf{L}}_1^{\pm}(\mathbf{s},x_3) = \frac{1}{\sqrt{2}}\begin{pmatrix} \frac{\sqrt{\mu s_3}}{s_0} & -\frac{s_1 s_2}{s_0\sqrt{\mathcal{E}s_3}} \\ 0 & \frac{s_0}{\sqrt{\mathcal{E}s_3}} \end{pmatrix}, \quad \tilde{\mathbf{L}}_2^{\pm}(\mathbf{s},x_3) = \pm\frac{1}{\sqrt{2}}\begin{pmatrix} \frac{s_0}{\sqrt{\mu s_3}} & 0 \\ \frac{s_1 s_2}{s_0\sqrt{\mu s_3}} & \frac{\sqrt{\mathcal{E}s_3}}{s_0} \end{pmatrix}, \tag{A19}$$

$$\tilde{\mathbf{\Lambda}}^{\pm}(\mathbf{s},x_3) = \pm i\omega\begin{pmatrix} s_3 & 0 \\ 0 & s_3 \end{pmatrix}, \quad s_0(\mathbf{s},x_3) = \sqrt{\frac{1}{c^2(x_3)} - s_2^2}, \tag{A20}$$

and $s_3(\mathbf{s},x_3)$ defined as in equation (A16), but with $c(x_3)$ defined as $c(x_3) = 1/\sqrt{\mathcal{E}(x_3)\mu(x_3)}$ for $x_3 = \pm x_{3,1}$.

For elastodynamic waves the sub-matrices of $\tilde{\mathbf{L}}$ and $\tilde{\mathbf{\Lambda}}$ are

$$\tilde{\mathbf{L}}_1^{\pm}(\mathbf{s},x_3) = \frac{1}{(2\rho)^{1/2}}\begin{pmatrix} \frac{s_1}{(s_3^P)^{1/2}} & -\frac{s_1(s_3^S)^{1/2}}{s_r} & -\frac{s_2}{c_S s_r (s_3^S)^{1/2}} \\ \frac{s_2}{(s_3^P)^{1/2}} & -\frac{s_2(s_3^S)^{1/2}}{s_r} & \frac{s_1}{c_S s_r (s_3^S)^{1/2}} \\ \pm(s_3^P)^{1/2} & \pm\frac{s_r}{(s_3^S)^{1/2}} & 0 \end{pmatrix}, \tag{A21}$$

$$\tilde{\mathbf{L}}_2^{\pm}(\mathbf{s},x_3) = \left(\frac{\rho}{2}\right)^{1/2} c_S^2 \begin{pmatrix} \pm 2s_1(s_3^P)^{1/2} & \mp\frac{s_1(c_S^{-2}-2s_r^2)}{s_r(s_3^S)^{1/2}} & \mp\frac{s_2(s_3^S)^{1/2}}{c_S s_r} \\ \pm 2s_2(s_3^P)^{1/2} & \mp\frac{s_2(c_S^{-2}-2s_r^2)}{s_r(s_3^S)^{1/2}} & \pm\frac{s_1(s_3^S)^{1/2}}{c_S s_r} \\ \frac{(c_S^{-2}-2s_r^2)}{(s_3^P)^{1/2}} & 2s_r(s_3^S)^{1/2} & 0 \end{pmatrix}, \tag{A22}$$

$$\tilde{\mathbf{\Lambda}}^{\pm}(\mathbf{s},x_3) = \pm i\omega\begin{pmatrix} s_3^P & 0 & 0 \\ 0 & s_3^S & 0 \\ 0 & 0 & s_3^S \end{pmatrix}, \tag{A23}$$

with $s_r = \sqrt{s_1^2 + s_2^2}$ and the vertical slownesses s_3^P and s_3^S defined as

$$s_3^{P,S}(\mathbf{s},x_3) = \sqrt{\frac{1}{c_{P,S}^2(x_3)} - s_\alpha s_\alpha}, \tag{A24}$$

where $c_P(x_3)$ and $c_S(x_3)$ are the P- and S-wave velocities, defined as $c_P(x_3) = \sqrt{(\lambda(x_3)+2\mu(x_3))/\rho(x_3)}$ and $c_S(x_3) = \sqrt{\mu(x_3)/\rho(x_3)}$, respectively, for $x_3 = \pm x_{3,1}$.

For all cases, matrix $\tilde{\mathbf{L}}(\mathbf{s},x_3)$ obeys the following symmetry relations

$$\tilde{\mathbf{L}}^t(-\mathbf{s},x_3)\mathbf{N}\tilde{\mathbf{L}}(\mathbf{s},x_3) = -\mathbf{N}, \tag{A25}$$

$$\tilde{\tilde{\mathbf{L}}}^{\dagger}(\mathbf{s},x_3)\mathbf{K}\tilde{\mathbf{L}}(\mathbf{s},x_3) = \mathbf{J}, \tag{A26}$$

for $x_3 = \pm x_{3,1}$. In equation (A26), $\tilde{\tilde{\mathbf{L}}}(\mathbf{s},x_3)$ is defined in the adjoint medium. In addition, for a $\mathcal{PT}$-symmetric medium we have

$$\tilde{\mathbf{L}}(\mathbf{s},-x_3) = \tilde{\mathbf{L}}^*(\mathbf{s},x_3), \tag{A27}$$

for $x_3 = \pm x_{3,1}$.

Appendix B. Detailed analysis of the boundary integrals

Here we present the details behind the analysis of the boundary integrals in section 4. We assume that at the boundary $\partial\mathbb{D}$ the medium is laterally invariant. The boundary integral in equation (16) consists of two integrals $\int_{\mathbb{R}^2} \mathbf{q}_A^t(\mathbf{x}_H,x_3)\mathbf{N}\mathbf{q}_B(\mathbf{x}_H,x_3)\mathrm{d}^2\mathbf{x}_H$, one for

Preprints (www.preprints.org) | NOT PEER-REVIEWED | Posted: 28 September 2022 doi:10.20944/preprints202209.0444.v1

for $x_3 = -x_{3,1}$ and one for $x_3 = x_{3,1}$. Using the spatial Fourier transform of equation (78) and Parseval's theorem, we obtain for these integrals

$$\int_{\mathbb{R}^2} \mathbf{q}_A^t(\mathbf{x}_\mathrm{H}, x_3)\mathbf{N}\mathbf{q}_B(\mathbf{x}_\mathrm{H}, x_3)\mathrm{d}^2\mathbf{x}_\mathrm{H} = \frac{\omega^2}{4\pi^2}\int_{\mathbb{R}^2} \tilde{\mathbf{q}}_A^t(-\mathbf{s}, x_3)\mathbf{N}\tilde{\mathbf{q}}_B(\mathbf{s}, x_3)\mathrm{d}^2\mathbf{s}, \tag{A28}$$

for $x_3 = -x_{3,1}$ and $x_3 = x_{3,1}$. Applying the spatial Fourier transform to equations (21) and (22), we obtain

$$\tilde{\mathbf{q}}_A(\mathbf{s}, x_3) = \tilde{\mathbf{L}}(\mathbf{s}, x_3)\tilde{\mathbf{p}}_A(\mathbf{s}, x_3), \tag{A29}$$
$$\tilde{\mathbf{q}}_B(\mathbf{s}, x_3) = \tilde{\mathbf{L}}(\mathbf{s}, x_3)\tilde{\mathbf{p}}_B(\mathbf{s}, x_3), \tag{A30}$$

with

$$\tilde{\mathbf{p}}_{A,B}(\mathbf{s}, x_3) = \begin{pmatrix} \tilde{\mathbf{p}}^+_{A,B}(\mathbf{s}, x_3) \\ \tilde{\mathbf{p}}^-_{A,B}(\mathbf{s}, x_3) \end{pmatrix}, \tag{A31}$$

where $\tilde{\mathbf{p}}^+_{A,B}(\mathbf{s}, x_3)$ and $\tilde{\mathbf{p}}^-_{A,B}(\mathbf{s}, x_3)$ are downgoing and upgoing plane-wave fields in states A and B at $x_3 = -x_{3,1}$ and $x_3 = x_{3,1}$. Note that $\tilde{\mathbf{L}}(\mathbf{s}, x_3)$ in equations (A29) and (A30) is without subscript A or B, which implies that we assume that the medium parameters at $\partial\mathbb{D}$ in both states are identical. Matrix $\tilde{\mathbf{L}}(\mathbf{s}, x_3)$ is given for a number of situations in Appendix A. Substitution of equations (A29) and (A30) into the right-hand side of equation (A28) gives

$$\int_{\mathbb{R}^2} \mathbf{q}_A^t(\mathbf{x}_\mathrm{H}, x_3)\mathbf{N}\mathbf{q}_B(\mathbf{x}_\mathrm{H}, x_3)\mathrm{d}^2\mathbf{x}_\mathrm{H} = \frac{\omega^2}{4\pi^2}\int_{\mathbb{R}^2} \tilde{\mathbf{p}}_A^t(-\mathbf{s}, x_3)\tilde{\mathbf{L}}^t(-\mathbf{s}, x_3)\mathbf{N}\tilde{\mathbf{L}}(\mathbf{s}, x_3)\tilde{\mathbf{p}}_B(\mathbf{s}, x_3)\mathrm{d}^2\mathbf{s}, \tag{A32}$$

for $x_3 = \pm x_{3,1}$. Using symmetry relation (A25) this yields

$$\int_{\mathbb{R}^2} \mathbf{q}_A^t(\mathbf{x}_\mathrm{H}, x_3)\mathbf{N}\mathbf{q}_B(\mathbf{x}_\mathrm{H}, x_3)\mathrm{d}^2\mathbf{x}_\mathrm{H} = -\frac{\omega^2}{4\pi^2}\int_{\mathbb{R}^2} \tilde{\mathbf{p}}_A^t(-\mathbf{s}, x_3)\mathbf{N}\tilde{\mathbf{p}}_B(\mathbf{s}, x_3)\mathrm{d}^2\mathbf{s}, \tag{A33}$$

for $x_3 = \pm x_{3,1}$. Applying Parseval's theorem to the right-hand side and combining the integrals for $x_3 = \pm x_{3,1}$, finally yields

$$\int_{\partial\mathbb{D}} \mathbf{q}_A^t(\mathbf{x})\mathbf{N}\mathbf{q}_B(\mathbf{x})n_3\mathrm{d}^2\mathbf{x}_\mathrm{H} = -\int_{\partial\mathbb{D}} \mathbf{p}_A^t(\mathbf{x})\mathbf{N}\mathbf{p}_B(\mathbf{x})n_3\mathrm{d}^2\mathbf{x}_\mathrm{H}. \tag{A34}$$

This is equation (23) in the main text, which holds when the medium parameters at $\partial\mathbb{D}$ in state A are the same as those in state B. Next, for the two integrals in the boundary integral in equation (17) we obtain, analogous to equation (A28),

$$\int_{\mathbb{R}^2} \mathbf{q}_A^\dagger(-\mathbf{x}_\mathrm{H}, -x_3)\mathbf{N}\mathbf{q}_B(\mathbf{x}_\mathrm{H}, x_3)\mathrm{d}^2\mathbf{x}_\mathrm{H} = \frac{\omega^2}{4\pi^2}\int_{\mathbb{R}^2} \tilde{\mathbf{q}}_A^\dagger(-\mathbf{s}, -x_3)\mathbf{N}\tilde{\mathbf{q}}_B(\mathbf{s}, x_3)\mathrm{d}^2\mathbf{s}, \tag{A35}$$

for $x_3 = -x_{3,1}$ and $x_3 = x_{3,1}$. Substitution of equations (A29) and (A30) into the right-hand side of equation (A35), using the $\mathcal{PT}$-symmetry relation of equation (A27), followed by symmetry relation (A25), applying Parseval's theorem to the right-hand side and combining the integrals for $x_3 = \pm x_{3,1}$, yields

$$\int_{\partial\mathbb{D}} \mathbf{q}_A^\dagger(-\mathbf{x})\mathbf{N}\mathbf{q}_B(\mathbf{x})n_3\mathrm{d}^2\mathbf{x}_\mathrm{H} = -\int_{\partial\mathbb{D}} \mathbf{p}_A^\dagger(-\mathbf{x})\mathbf{N}\mathbf{p}_B(\mathbf{x})n_3\mathrm{d}^2\mathbf{x}_\mathrm{H}. \tag{A36}$$

This is equation (24) in the main text, which only holds when the medium parameters at the boundary have $\mathcal{PT}$-symmetry and are the same in states A and B.

Next, we replace equation (A29) by

$$\tilde{\mathbf{q}}_A(\mathbf{s}, x_3) = \tilde{\tilde{\mathbf{L}}}(\mathbf{s}, x_3)\tilde{\mathbf{p}}_A(\mathbf{s}, x_3), \tag{A37}$$

Preprints (www.preprints.org) | NOT PEER-REVIEWED | Posted: 28 September 2022 doi:10.20944/preprints202209.0444.v1

which is the spatial Fourier transform of equation (25), where $\tilde{\mathbf{L}}(\mathbf{s}, x_3)$ is defined in the adjoint medium at $\partial\mathbb{D}$. We use this for the analysis of the other boundary integrals. For the two integrals in the boundary integral in equation (18) we obtain

$$\int_{\mathbb{R}^2} \mathbf{q}_A^\dagger(\mathbf{x}_\mathrm{H}, x_3)\mathbf{K}\mathbf{q}_B(\mathbf{x}_\mathrm{H}, x_3)\mathrm{d}^2\mathbf{x}_\mathrm{H} = \frac{\omega^2}{4\pi^2}\int_{\mathbb{R}^2} \tilde{\mathbf{q}}_A^\dagger(\mathbf{s}, x_3)\mathbf{K}\tilde{\mathbf{q}}_B(\mathbf{s}, x_3)\mathrm{d}^2\mathbf{s}, \tag{A38}$$

for $x_3 = -x_{3,1}$ and $x_3 = x_{3,1}$. Substitution of equations (A30) and (A37) into the right-hand side of equation (A38), using symmetry relation (A26), applying Parseval's theorem to the right-hand side and combining the integrals for $x_3 = \pm x_{3,1}$, yields

$$\int_{\partial\mathbb{D}} \mathbf{q}_A^\dagger(\mathbf{x})\mathbf{K}\mathbf{q}_B(\mathbf{x})n_3\mathrm{d}^2\mathbf{x}_\mathrm{H} \quad = \quad \int_{\partial\mathbb{D}} \mathbf{p}_A^\dagger(\mathbf{x})\mathbf{J}\mathbf{p}_B(\mathbf{x})n_3\mathrm{d}^2\mathbf{x}_\mathrm{H}. \tag{A39}$$

This is equation (26) in the main text, which holds when the medium parameters at $\partial\mathbb{D}$ in state A are the adjoint of those in state B. Finally, for the two integrals in the boundary integral in equation (19) we obtain

$$\int_{\mathbb{R}^2} \mathbf{q}_A^t(-\mathbf{x}_\mathrm{H}, -x_3)\mathbf{K}\mathbf{q}_B(\mathbf{x}_\mathrm{H}, x_3)\mathrm{d}^2\mathbf{x}_\mathrm{H} = \frac{\omega^2}{4\pi^2}\int_{\mathbb{R}^2} \tilde{\mathbf{q}}_A^t(\mathbf{s}, -x_3)\mathbf{K}\tilde{\mathbf{q}}_B(\mathbf{s}, x_3)\mathrm{d}^2\mathbf{s}, \tag{A40}$$

for $x_3 = -x_{3,1}$ and $x_3 = x_{3,1}$. Substitution of equations (A30) and (A37) into the right-hand side of equation (A40), using the $\mathcal{PT}$-symmetry relation of equation (A27), followed by symmetry relation (A26), applying Parseval's theorem to the right-hand side and combining the integrals for $x_3 = \pm x_{3,1}$, yields

$$\int_{\partial\mathbb{D}} \mathbf{q}_A^t(-\mathbf{x})\mathbf{K}\mathbf{q}_B(\mathbf{x})n_3\mathrm{d}^2\mathbf{x}_\mathrm{H} \quad = \quad \int_{\partial\mathbb{D}} \mathbf{p}_A^t(-\mathbf{x})\mathbf{J}\mathbf{p}_B(\mathbf{x})n_3\mathrm{d}^2\mathbf{x}_\mathrm{H}. \tag{A41}$$

This is equation (27) in the main text, which only holds when the medium parameters at $\partial\mathbb{D}$ have $\mathcal{PT}$-symmetry and in state A they are the adjoint of those in state B.

References

1. Bender, C.M.; Boettcher, S. Real spectra in non-Hermitian Hamiltonians having $\mathcal{PT}$ symmetry. *Physical Review Letters* **1998**, *80*, 5243–5246.
2. Rüter, C.E.; Makris, K.G.; El-Ganainy, R.; Christodoulides, D.N.; Segev, M.; Kip, D. Observation of parity–time symmetry in optics. *Nature Physics* **2010**, *6*, 192–195.
3. Ge, L.; Chong, Y.D.; Stone, A.D. Conservation relations and anisotropic transmission resonances in one-dimensional $\mathcal{PT}$-symmetric photonic heterostructures. *Physical Review A* **2012**, *85*, 023802.
4. Özdemir, S.K.; Rotter, S.; Nori, F.; Yang, L. Parity–time symmetry and exceptional points in photonics. *Nature Materials* **2019**, *18*, 783–798.
5. Christensen, J.; Willatzen, M.; Velasco, V.R.; Lu, M.H. Parity-time synthetic phononic media. *Physical Review Letters* **2016**, *116*, 207601.
6. Yi, J.; Negahban, M.; Li, Z.; Su, X.; Xia, R. Conditionally extraordinary transmission in periodic parity-time symmetric phononic crystals. *International Journal of Mechanical Sciences* **2019**, *163*, 105134.
7. Yang, H.; Zhang, X.; Liu, Y.; Yao, Y.; Wu, F.; Zhao, D. Novel acoustic flat focusing based on the asymmetric response in parity-time-symmetric phononic crystals. *Scientific Reports* **2019**, *9*, 10048.
8. Zhu, X.; Ramezani, H.; Shi, C.; Zhu, J.; Zhang, X. $\mathcal{PT}$-symmetric acoustics. *Physical Review X* **2014**, *4*, 031042.
9. Fleury, R.; Sounas, D.; Alù, A. An invisible acoustic sensor based on parity-time symmetry. *Nature Communications* **2015**, *6*, 5905.
10. Fleury, R.; Sounas, D.L.; Alù, A. Parity-time symmetry in acoustics: Theory, devices, and potential applications. *IEEE Journal of Selected Topics in Quantum Electronics* **2016**, *22*, 5000809.
11. Ramezani, H.; Kottos, T.; El-Ganainy, R.; Christodoulides, D.N. Unidirectional non-linear $\mathcal{PT}$-symmetric optical structures. *Physical Review A* **2010**, *82*, 043803.
12. Bojarski, N.N. Generalized reaction principles and reciprocity theorems for the wave equations, and the relationship between the time-advanced and time-retarded fields. *Journal of the Acoustical Society of America* **1983**, *74*, 281–285.
13. de Hoop, A.T. Time-domain reciprocity theorems for electromagnetic fields in dispersive media. *Radio Science* **1987**, *22*, 1171–1178.
14. de Hoop, A.T. Time-domain reciprocity theorems for acoustic wave fields in fluids with relaxation. *Journal of the Acoustical Society of America* **1988**, *84*, 1877–1882.

15. Huignard, J.P.; Marrakchi, A. Coherent signal beam amplification in two-wave mixing experiments with photorefractive $Bi_{12}SiO_{20}$ crystals. *Optics Communications* **1981**, *38*, 249–254.
16. Hutson, A.R.; McFee, J.H.; White, D.L. Ultrasonic amplification in CdS. *Physical Review Letters* **1961**, *7*, 237–239.
17. Moleron, M.; van Manen, D.J.; Robertsson, J.O.A. Mimicking metamaterial functionalities in an immersive laboratory with exact boundary conditions. In Proceedings of the META'17 Incheon - Korea, 2017, pp. 1437–1438.
18. Van Manen, D.J.; Moleron, M.; Thomsen, H.R.; Börsing, N.; Becker, T.S.; Haberman, M.R.; Robertsson, J.O.A. Immersive boundary conditions for meta-material experimentation. *Journal of the Acoustical Society of America* **2019**, *146*, 2786.
19. Börsing, N.; Becker, T.S.; Curtis, A.; van Manen, D.J.; Haag, T.; Robertsson, J.O.A. Cloaking and holography experiments using immersive boundary conditions. *Physical Review Applied* **2019**, *12*, 024011.
20. Becker, T.S.; Börsing, N.; Haag, T.; Bärlocher, C.; Donahue, C.M.; Curtis, A.; Robertsson, J.O.A.; van Manen, D.J. Real-time immersion of physical experiments in virtual wave-physics domains. *Physical Review Applied* **2020**, *13*, 064061.
21. Van Manen, D.J.; Robertsson, J.O.A.; Curtis, A. Exact wave field simulation for finite-volume scattering problems. *Journal of the Acoustical Society of America* **2007**, *122*, EL115–EL121.
22. Vasmel, M.; Robertsson, J.O.A.; van Manen, D.J.; Curtis, A. Immersive experimentation in a wave propagation laboratory. *Journal of the Acoustical Society of America* **2013**, *134*, EL492–EL498.
23. Li, X.; Koene, E.; van Manen, D.J.; Robertsson, J.; Curtis, A. Elastic immersive wavefield modelling. *Journal of Computational Physics* **2022**, *451*, 110826.
24. Rayleigh, J.W.S. *The theory of sound. Volume II*; Dover Publications, Inc. (Reprint 1945), 1878.
25. Lorentz, H.A. The theorem of Poynting concerning the energy in the electromagnetic field and two general propositions concerning the propagation of light. *Verslagen der Afdeeling Natuurkunde van de Koninklijke Akademie van Wetenschappen* **1895**, *4*, 176–187.
26. Knopoff, L.; Gangi, A.F. Seismic reciprocity. *Geophysics* **1959**, *24*, 681–691.
27. de Hoop, A.T. An elastodynamic reciprocity theorem for linear, viscoelastic media. *Applied Scientific Research* **1966**, *16*, 39–45.
28. Knopoff, L. Diffraction of elastic waves. *Journal of the Acoustical Society of America* **1956**, *28*, 217–229.
29. de Hoop, A.T. Representation theorems for the displacement in an elastic solid and their applications to elastodynamic diffraction theory. PhD thesis, Delft University of Technology, Delft, 1958.
30. Gangi, A.F. A derivation of the seismic representation theorem using seismic reciprocity. *Journal of Geophysical Research* **1970**, *75*, 2088–2095.
31. Pao, Y.H.; Varatharajulu, V. Huygens' principle, radiation conditions, and integral formulations for the scattering of elastic waves. *Journal of the Acoustical Society of America* **1976**, *59*, 1361–1371.
32. Wapenaar, K.; Thorbecke, J.; Draganov, D. Relations between reflection and transmission responses of three-dimensional inhomogeneous media. *Geophysical Journal International* **2004**, *156*, 179–194.
33. Broggini, F.; Snieder, R. Connection of scattering principles: a visual and mathematical tour. *European Journal of Physics* **2012**, *33*, 593–613.
34. Wapenaar, K.; Broggini, F.; Slob, E.; Snieder, R. Three-dimensional single-sided Marchenko inverse scattering, data-driven focusing, Green's function retrieval, and their mutual relations. *Physical Review Letters* **2013**, *110*, 084301.
35. Slob, E.; Wapenaar, K.; Broggini, F.; Snieder, R. Seismic reflector imaging using internal multiples with Marchenko-type equations. *Geophysics* **2014**, *79*, S63–S76.
36. Gilbert, F.; Backus, G.E. Propagator matrices in elastic wave and vibration problems. *Geophysics* **1966**, *31*, 326–332.
37. Kennett, B.L.N. The connection between elastodynamic representation theorems and propagator matrices. *Bulletin of the Seismological Society of America* **1972**, *62*, 973–983.
38. Kennett, B.L.N. Seismic waves in laterally inhomogeneous media. *Geophysical Journal of the Royal Astronomical Society* **1972**, *27*, 301–325.
39. Woodhouse, J.H. Surface waves in a laterally varying layered structure. *Geophysical Journal of the Royal Astronomical Society* **1974**, *37*, 461–490.
40. Haines, A.J. Multi-source, multi-receiver synthetic seismograms for laterally heterogeneous media using F-K domain propagators. *Geophysical Journal International* **1988**, *95*, 237–260.
41. Wapenaar, K. Unified matrix-vector wave equation, reciprocity and representations. *Geophysical Journal International* **2019**, *216*, 560–583.
42. Ursin, B. Review of elastic and electromagnetic wave propagation in horizontally layered media. *Geophysics* **1983**, *48*, 1063–1081.
43. Løseth, L.O.; Ursin, B. Electromagnetic fields in planarly layered anisotropic media. *Geophysical Journal International* **2007**, *170*, 44–80.
44. Auld, B.A. General electromechanical reciprocity relations applied to the calculation of elastic wave scattering coefficients. *Wave Motion* **1979**, *1*, 3–10.
45. Pride, S.R.; Haartsen, M.W. Electroseismic wave properties. *Journal of the Acoustical Society of America* **1996**, *100*, 1301–1315.
46. de Hoop, A.T. *Handbook of radiation and scattering of waves*; Academic Press, London, 1995.
47. Achenbach, J.D. *Reciprocity in elastodynamics*; Cambridge University Press, Cambridge, 2003.
48. Haines, A.J.; de Hoop, M.V. An invariant imbedding analysis of general wave scattering problems. *J. Math. Phys.* **1996**, *37*, 3854–3881.

49. Wapenaar, C.P.A. Reciprocity theorems for two-way and one-way wave vectors: a comparison. *Journal of the Acoustical Society of America* **1996**, *100*, 3508–3518.
50. Wapenaar, K. Reciprocity and representation theorems for flux- and field-normalised decomposed wave fields. *Advances in Mathematical Physics* **2020**, *2020*, 9540135.
51. Wapenaar, C.P.A.; Dillen, M.W.P.; Fokkema, J.T. Reciprocity theorems for electromagnetic or acoustic one-way wave fields in dissipative inhomogeneous media. *Radio Science* **2001**, *36*, 851–863.
52. Kennett, B.L.N. *Seismic wave propagation in stratified media*; Cambridge University Press, 1983.
53. Porter, R.P. Diffraction-limited, scalar image formation with holograms of arbitrary shape. *Journal of the Optical Society of America* **1970**, *60*, 1051–1059.
54. Oristaglio, M.L. An inverse scattering formula that uses all the data. *Inverse Problems* **1989**, *5*, 1097–1105.
55. Porter, R.P.; Devaney, A.J. Holography and the inverse source problem. *Journal of the Optical Society of America* **1982**, *72*, 327–330.
56. Devaney, A.J. A filtered backpropagation algorithm for diffraction tomography. *Ultrasonic Imaging* **1982**, *4*, 336–350.
57. Bleistein, N. *Mathematical methods for wave phenomena*; Academic Press, Inc., Orlando, 1984.
58. Schneider, W.A. Integral formulation for migration in two and three dimensions. *Geophysics* **1978**, *43*, 49–76.
59. Berkhout, A.J. *Seismic Migration. Imaging of acoustic energy by wave field extrapolation. A. Theoretical aspects*; Elsevier, 1982.
60. Maynard, J.D.; Williams, E.G.; Lee, Y. Nearfield acoustic holography: I. Theory of generalized holography and the development of NAH. *Journal of the Acoustical Society of America* **1985**, *78*, 1395–1413.
61. Esmersoy, C.; Oristaglio, M. Reverse-time wave-field extrapolation, imaging, and inversion. *Geophysics* **1988**, *53*, 920–931.
62. Lindsey, C.; Braun, D.C. Principles of seismic holography for diagnostics of the shallow subphotosphere. *The Astrophysical Journal Supplement Series* **2004**, *155*, 209–225.
63. Fink, M.; Prada, C. Acoustic time-reversal mirrors. *Inverse Problems* **2001**, *17*, R1–R38.
64. Derode, A.; Larose, E.; Tanter, M.; de Rosny, J.; Tourin, A.; Campillo, M.; Fink, M. Recovering the Green's function from field-field correlations in an open scattering medium (L). *Journal of the Acoustical Society of America* **2003**, *113*, 2973–2976.
65. Wapenaar, K. Synthesis of an inhomogeneous medium from its acoustic transmission response. *Geophysics* **2003**, *68*, 1756–1759.
66. Weaver, R.L.; Lobkis, O.I. Diffuse fields in open systems and the emergence of the Green's function (L). *Journal of the Acoustical Society of America* **2004**, *116*, 2731–2734.
67. Weaver, R.L.; Lobkis, O.I. Ultrasonics without a source: Thermal fluctuation correlations at MHz frequencies. *Physical Review Letters* **2001**, *87*, 134301.
68. Campillo, M.; Paul, A. Long-range correlations in the diffuse seismic coda. *Science* **2003**, *299*, 547–549.
69. Marchenko, V.A. Reconstruction of the potential energy from the phases of the scattered waves (in Russian). *Doklady Akademii Nauk SSSR* **1955**, *104*, 695–698.
70. Wapenaar, K.; Thorbecke, J.; van der Neut, J.; Broggini, F.; Slob, E.; Snieder, R. Marchenko imaging. *Geophysics* **2014**, *79*, WA39–WA57.
71. Broggini, F.; Snieder, R.; Wapenaar, K. Data-driven wavefield focusing and imaging with multidimensional deconvolution: Numerical examples for reflection data with internal multiples. *Geophysics* **2014**, *79*, WA107–WA115.
72. Wapenaar, K.; Slob, E. On the Marchenko equation for multicomponent single-sided reflection data. *Geophysical Journal International* **2014**, *199*, 1367–1371.
73. Ravasi, M.; Vasconcelos, I.; Kritski, A.; Curtis, A.; da Costa Filho, C.A.; Meles, G.A. Target-oriented Marchenko imaging of a North Sea field. *Geophysical Journal International* **2016**, *205*, 99–104.
74. Brackenhoff, J.; Thorbecke, J.; Wapenaar, K. Virtual sources and receivers in the real Earth: Considerations for practical applications. *Journal of Geophysical Research* **2019**, *124*, 11,802–11,821.
75. Elison, P.; Dukalski, M.S.; de Vos, K.; van Manen, D.J.; Robertsson, J.O.A. Data-driven control over short-period internal multiples in media with a horizontally layered overburden. *Geophysical Journal International* **2020**, *221*, 769–787.
76. Ravasi, M.; Vasconcelos, I. An open-source framework for the implementation of large-scale integral operators with flexible, modern high-performance computing solutions: Enabling 3D Marchenko imaging by least-squares inversion. *Geophysics* **2021**, *86*, WC177–WC194.
77. Slob, E. Green's function retrieval and Marchenko imaging in a dissipative acoustic medium. *Physical Review Letters* **2016**, *116*, 164301.
78. Stoffa, P.L. *Tau-p - A plane wave approach to the analysis of seismic data*; Kluwer Academic Publishers: Dordrecht, 1989.
79. Corones, J.P. Bremmer series that correct parabolic approximations. *J. Math. Anal. Appl.* **1975**, *50*, 361–372.
80. Fishman, L.; McCoy, J.J. Derivation and application of extended parabolic wave theories. I. The factorized Helmholtz equation. *J. Math. Phys.* **1984**, *25*, 285–296.
81. Wapenaar, C.P.A.; Berkhout, A.J. *Elastic wave field extrapolation*; Elsevier, Amsterdam, 1989.
82. de Hoop, M.V. Generalization of the Bremmer coupling series. *J. Math. Phys.* **1996**, *37*, 3246–3282.
83. Messiah, A. *Quantum mechanics, Volume I*; North-Holland Publishing Company, Amsterdam, 1961.
84. Merzbacher, E. *Quantum mechanics*; John Wiley and Sons, Inc., New York, 1961.